CHARACTERIZATION, ANTIBACTERIAL ACTIVITY AND CYTOTOXICITY OF COTTON FABRIC COATED WITH METAL NANOPARTICLES

2023
MASTER THESIS
BIOMEDICAL ENGINEERING

Ladan ABDI ATTEYE

Thesis Advisor
Assist. Prof. Dr. Ammar ZIDANOĞLU

CHARACTERIZATION, ANTIBACTERIAL ACTIVITY AND CYTOTOXICITY OF COTTON FABRIC COATED WITH METAL NANOPARTICLES

Ladan ABDI ATTEYE

Thesis Advisor
Assist. Prof. Dr. Ammar ZIDANOĞLU

T.C
Karabük University
Institute of Graduate Programs
Department of Biomedical Engineering
Prepared as
Master Thesis

KARABÜK
June 2023

I certify that in my opinion the thesis submitted by Ladan ABDI ATTEYE titled "CHARACTERIZATION, ANTIBACTERIAL ACTIVITY, AND CYTOTOXICITY OF COTTON FABRIC COATED WITH METAL NANOPARTICLES" is fully adequate in scope and in quality as a thesis for the degree of Master of Science.

Assist. Prof. Dr. Ammar ZIDANOĞLU .....
Thesis Advisor, Department of Biomedical Engineering

This thesis is accepted by the examining committee with a unanimous vote in the Department of Biomedical Engineering as a Master of Science thesis. 15/06/2023

Examining Committee Members (Institutions)	Signature
Chairman : Assoc. Prof. Dr. Hacı Mehmet KAYILI (KBU)	.....
Member : Assist. Prof. Dr. Ammar ZIDANOĞLU (KBU)	….....
Member : Assist. Prof. Dr. İsmail SEÇKİN (ATA)	.....

The degree of Master of Science by the thesis submitted is approved by the Administrative Board of the Institute of Graduate Programs, Karabuk University.

Prof. Dr. Müslüm KUZU .....
Director of Graduate School of Education

I declare that all information contained in this document has been obtained and presented in accordance with academic rules and ethics. I also declare that, in accordance with these rules and conduct, I have cited and referenced all non-original material and results in this document.

Ladan ABDI ATTEYE

ABSTRACT

M. Sc. Thesis

CHARACTERIZATION, ANTIBACTERIAL ACTIVITY, AND CYTOTOXICITY OF COTTON FABRIC COATED WITH METAL NANOPARTICLES

Ladan ABDI ATTEYE

Karabük University
Institute of Graduate Programs
The Department of Biomedical Engineering

Thesis Advisor:
Assist. Prof. Dr. Ammar ZIDANOĞLU
June 2023, 77 pages

In recent years, one of the fastest-growing industries has been the antibacterial textile business, which has greatly benefited from nanoparticles due to their unique and helpful properties for high-performance textiles. In this research project, fabric cotton is coated with different fractions of metal nanoparticles like lanthanum (La), cobalt (Co), and gallium (Ga) using the co-precipitation method. The prepared composites were characterized using X-ray diffraction (XRD), scanning electron microscopy (SEM), energy-dispersive X-ray (EDX), Fourier transform infrared spectroscopy (FTIR), and thermogravimetric analysis (TGA). According to the findings of the XRD analysis, cellulose was transformed into cellulose II, and Co and La were not detected in the XRD pattern. The results of the SEM analysis showed that nanometal particles were detected on the cotton's surface. EDX further investigated the structure of the nanometal particles. The starching and bending modes of the functional groups were

detected using FTIR. The thermal stability of the prepared composites was studied using TGA. The in vitro antibacterial activity of the cotton-metal composites was studied using Staphylococcus aureus bacteria. The disk diffusion method showed that the composites had no antibacterial activity, while the dilution method showed antibacterial activity. A deep blue assay was used to evaluate the cytotoxicity behaviour of the prepared materials when cultured with a mouse fibroblast cell line for 24 hours. The results showed that the cotton-0.04M metal composite materials were cytocompatible and had no adverse effect.

Key Words : Cotton, Nanometals, Coating, Antibacterial Textiles, Cytotoxicity
Science Code : 92503

ÖZET

Yüksek Lisans Tezi

METAL NANOPARTİKÜLLER İLE KAPLANMIŞ PAMUKLU KUMAŞIN KARAKTERİZASYONU, ANTİBAKTERİYEL AKTİVİTESİVE SİTOTOKSİSİTESİ

Ladan ABDI ATTEYE

Karabük Üniversitesi
Lisansüstü Eğitim Enstitüsü
Biyomedikal Mühendisliği Anabilim Dalı

Tez Danışmanı:
Dr. Öğr. Üyesi Ammar ZIDANOĞLU
Haziran 2023, 77 sayfa

Son yıllarda, en hizli büyüyen sektörlerden biri antibakteriyel tekstil sektörü olmuştur, Yüksek performanslı tekstiller benzersiz ve faydalı özellikleri nedeniyle nanopartiküllerden büyük ölçüde yararlanır. Bu araştırma projesinde, pamuklu kumaş, birlikte çökeltme yöntemi kullanılarak lantan (La), kobalt (Co) ve galyum (Ga) gibi farklı metal nanopartikül fraksiyonları ile kaplanmıştır. Hazırlanan kompozitler X-ışını kırınımı (XRD), taramalı elektron mikroskobu (SEM), enerji dağılımlı X-ışını (EDX), Fourier dönüşümlü kızılötesi spektroskopisi (FTIR) ve termogravimetrik analiz (TGA) kullanılarak karakterize edilmiştir.XRD analizi bulgularına göre, selüloz selüloz II'ye dönüşmüş ve XRD deseninde La ve La tespit edilmemiştir.SEM analizinin sonuçları pamuk yüzeyinde nanometal partiküllerin tespit edildiğini göstermiştir. EDX ayrıca nanometal partiküllerin yapısını da araştırmıştır. Fonksiyonel grupların nişastalanma ve bükülme modları FTIR kullanılarak tespit

edilmiştir. Hazırlanan kompozitlerin termal kararlılığı TGA kullanılarak incelenmiştir. Pamuk-metal kompozitlerin in vitro antibakteriyel aktivitesi Staphylococcus aureus bakterisi kullanılarak incelenmiştir. Disk difüzyon yöntemi kompozitlerin antibakteriyel aktiviteye sahip olmadığını gösterirken, seyreltme yöntemi antibakteriyel aktivite göstermiştir. Bir fare fibroblast hücre hattı ile 24 saat boyunca kültürlendiğinde hazırlanan malzemelerin sitotoksisite davranışını değerlendirmek için bir derin mavi testi kullanılmıştır. Sonuçlar, pamuk-0.04M metal kompozit malzemelerin sitouyumlu olduğunu ve herhangi bir olumsuz etkisinin olmadığını göstermiştir.

Anahtar Kelimeler **:** Pamuk, Nanometallar; Kaplama; Antibakteriyel Tekstiller, Sitotoksisite.

Bilim kodu **:** 92503

ACKNOWLEDGEMENT

Being one of the news merging concepts, the concern research study attached to my thesis was not only rich in experience but also motivational. Its success converges the results of numerous contributions, encouragement, and mostly guidelines. The board features were narrowed down by guidelines, the difficult yet confusing situations were clarified by contributions and encouragements.

Taking this opportunity, I would like to highlight and express my gratitude as well as my appreciation towards people who contributed directly or indirectly.

My deepest appreciation goes to my research supervisor, Assist. Prof. Dr. Ammar Zeidan Ghailan ALSHEMARY. He’s distinguished sense of leadership and guidance were unique. Accounting for a supportive figure, he was always present, responsive.

In addition, my recognition goes to my parents, whom encouragement played a distinctive role through the whole process in this project. I would also like to express my deepest gratitude to Ameer Al-humairi for his rightous guidance.

CONTENTS

Page

Page

Page

LIST OF FIGURES

Page

Page

LIST OF TABLES

Page

SYMBOLS AND ABBREVIATIONS

SYMBOLS

°	: Degree
°C	: The degree Celsius

ABBREVIATIONS

$C_6H_8O_6$	: Ascorbic acid
Ag	: Silver
$Co(NO_3)_2$	: Cobalt nitrate
Cu	: Copper
Ce	: Cerium
Eu	: Europium
EDX	: Energy-dispersive X-ray
$Ga(NO_3)_3$	: Gallium nitrate
Au	: Gold
$La(NO_3)_3$	: Lanthanum(III) nitrate
Lu	: Lutetium
NP_S	: Nanoparticle
Pr	: Praseodymium
REEs	: Rare Earth Elements
SEM	: Scanning Electron Microscopy
NaOH	: Sodium hydroxide
SBF	: Simulated Body Fluid
Sm	: Samarium
Ti	: Titanium
TiO_2	: Titanium dioxide
TGA	: Thermo Gravimetric Analysis
XRD	: X-Ray Diffraction

Zn : Zinc

ZnO : Zinc oxide

Y : Yttrium

PART 1

INTRODUCTION

1.1. SKIN

The skin, biggest mammal organ, is an essential component of the body's immune system and plays an important protective role. It is the initial defence against the outside environment and can fend off diverse opportunistic organisms [1]. It is made of three layers, epidermis, dermis and hypodermis. The thickness of the epidermis, which is the most superficial layer of the skin, varies depending on the location of the skin on the body. The depths of the dermis also vary based mostly on the body's position, and the dermis is attached to an underlying hypodermis. The epidermis is composed of five sublayers (Stratum basale, Stratum spinosum, Stratum granulosum, Stratum lucidum, and Stratum corneum), followed by the dermis, its primary function is to support and maintain the epidermis, elastin and collagen fibers are the main constituent of the dermis and it is made of two sub-layers (papillary layer, the reticular layer). The hypodermis is a layer of fat and connective tissue that encloses larger blood vessels and nerves. At last, the hypodermis of a substantial portion of fat cells for acting as a shock absorber for blood arteries and nerve terminals [2], as illustrated in figure1.1.

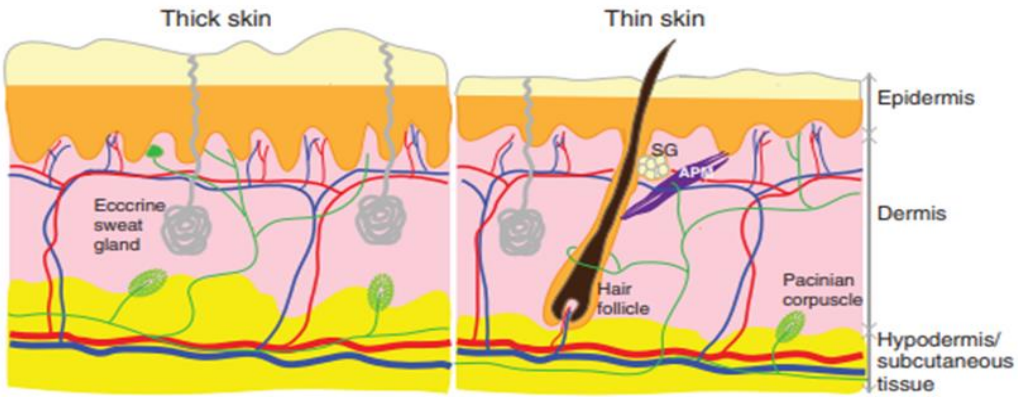

Figure 1.1. Layers of the skin [3].

1.1.1. Microbial Skin Infection

Defending against microbial invasion, the skin is a formidable barrier, while numerous bacteria can make contact with or live on the skin's surface [3]. The vast majority of these bacteria are unable to cause an illness on their own. Still, local alterations in the microenvironment can affect the layout of the community, leading to an imbalance in the microbiome. The bacteria on the skin can be subdivided into commensal, part of a stable community of microorganisms, not detrimental to the host (see in table1.1) or temporary microorganisms that do not constantly settle on the skin [4].

Table 1.1. Example of commensal bacteria [5].

Main group Bacteria	**Percentages (%)**
Actinobacteria	51.8%
Firmicutes	24.4%
Proteobacteria	16.5%
Bacteroidetes	6.3%

A constantly regenerating organ skin dynamically regulates the body's inside-outside connections and plays an essential role in the immune system's defences [6]. *Staphylococcus*, *Micrococcus*, and *Corynebacterium spp* are a few examples of gram-positive bacteria Commonly diagnosed as pathogens on the skin. To be pathogenic, they need to be capable of adhering to the skin; a reported way of adhesion is related to surface charge physicochemical phenomena that are crucial to the adherence process of bacteria. Rapid and secure adhesion of bacteria to positively charged surfaces is accompanied by electrostatic repulsion of cells from negatively charged surfaces. Various ligands (carboxylate, hydroxyl, phosphate, and amine moieties) are exposed on the bacterial cell wall's outermost layer, which could bind with substrates [7]. Several bacterial-associated proteins (lipo) teichoic polysaccharides were related to the bacteria's remarkable ability to adhere to surfaces [8].

1.2. FABRIC COTTON

Cotton is a natural textile fiber that comes from the seeds of the cotton plants, cotton plants are dicotyledons belonging to the family Malvaceae, tribe Hibicae and genus Gossypium, there are four different species of cotton that belong to the genus Gossypium. Cotton fibers contain more than 90% cellulose [10]. The purest natural form of this carbohydrate cellulose is a crystalline polymer of glucose that makes up the major structural constituent of the wall of many organisms, the formula of cellulose is $(C_{12}O_{22}H_{11})n$.

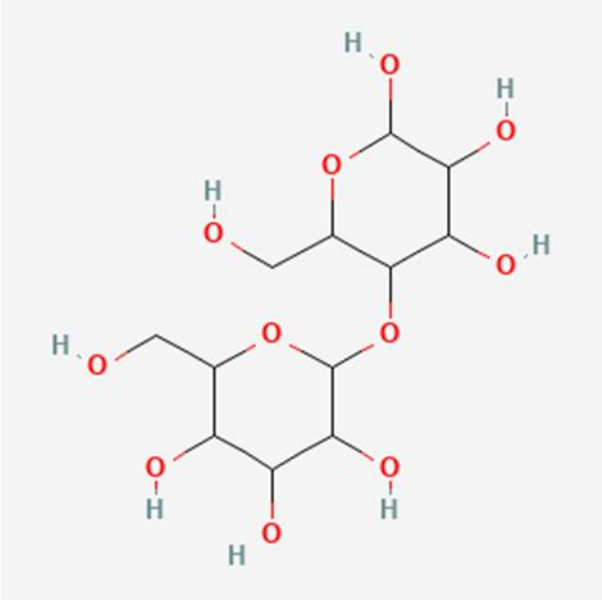

Figure 1.2. Chemical structure of Cellulose.

1.2.1. Cotton Fiber Structure

The cotton fibre's primary cell wall, particularly the cuticle's outer surface layer (which forms a protective film), significantly impacts fibre qualities, processing, and use due to its multilayered structure. The fibrillar structure of cotton includes a primary wall, secondary wall, lumen, Cellulose, hemicelluloses, pectin, proteins, and ions are the building blocks responsible for the structural integrity of the primary wall. Only crystalline cellulose is found in the secondary wall, which is extremely organized and

compact due to the orientation of the cellulose fibrils, which are parallel to one another [4].

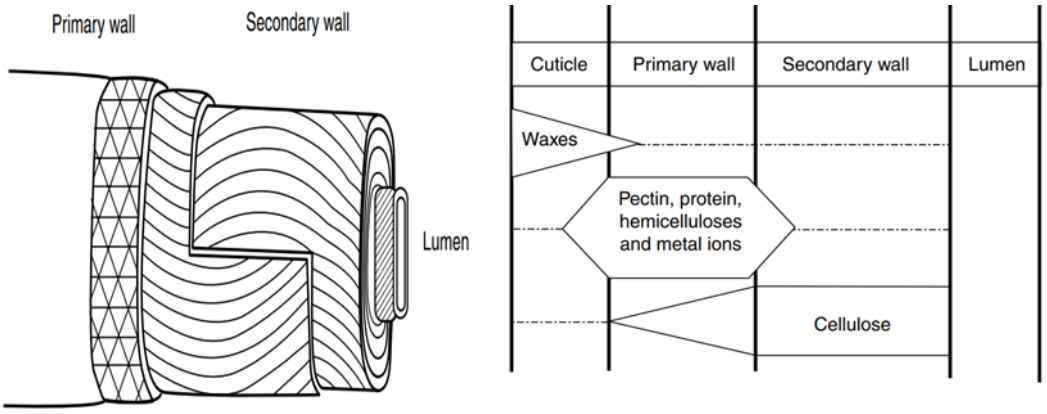

a) b)

Figure 1.3. a) Structure of cotton, and b) the non cellulosic part [12].

1.2.2. Cotton In Medical Field

Cotton's many medical and biological uses can be divided into the following two categories, the first category includes uses on the body itself, such as for treating wounds, administering drugs, treating dental problems, creating artificial tissues, and performing surgery, used in conjunction with antiseptic, disinfectant, cleaning, or even moisturizing products, the next category includes uses that are visible to the outside world, such as gowns, masks and uniforms, caps (medical attires), and pillowcases [4]. Cotton's diverse uses in the medical and private sectors stem from the fiber's inherent softness, absorbent capacity, and resistance to abrasion. Cotton's valuable qualities as a wound treatment material, gas permeability and high mechanical strength are two of its selling points. As a dressing for chronic and burn wounds, its ability to absorb wound fluid like blood and exudates is crucial since chronic and burn wounds tend to be very discharging, they require regular dressing changes that might add up in cost also its applicability is limited due to the fact that it does not possess antibacterial activity and bacterial proliferation is a high probability occurrence [5]. Pure cotton cannot be applied directly on the wounds, the wound may get even further infected due to the absence of a disinfecting agent and that's why the scientist's desire to create novel cotton-based biomaterials with expanded functionalities has only grown over the

years. Applying cotton treated with antibiotics to the skin can help stop the spread of bacteria and other potentially hazardous microorganisms, with little or no unacceptable side effects or toxicity to the treated area. Cotton can be coated with a substance of natural origin, semi-synthetic, or metallic, which is effective against microorganisms. Antimicrobial textiles are pretty valuable for today's world, particularly in settings such as hospitals, environments, and other locations that are prone to the growth of harmful microorganisms; both killing bacteria and preventing them from sticking to the surface are common mechanisms employed by antibacterial coatings.

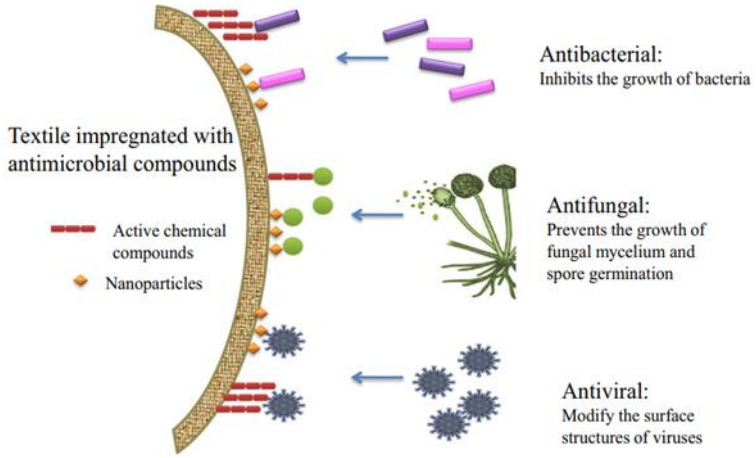

Figure 1.4. Graphic of a tissue coated with antimicrobial agent [11].

1.2.3. Non-Metallic Coating Agents

The base and coating materials are essential in the overall picture of things involving technology. An example of no metallic agent coated with is chitosan. The chitosan polysaccharide is obtained from chitin's deacetylation, which is the largest constituent of crustacean exoskeletons such as shrimp [12]. Chitosan's broad spectrum of activity and excellent death rate against gram-positive and gram-negative bacteria make it a popular choice as an antibacterial agent in textiles. Additionally, the antibacterial activities of textile material following chitosan treatment are impacted by several intrinsic and extrinsic parameters, including pH, microbe species, positive charge density, physical state, molecular weight, and degree of deacetylation of chitosan [13]. *S. aureus and E. coli* showed no resistance to untreated cotton fabric samples; nonetheless, chitosan-treated fabric samples showed a marked enhancement in

antibacterial ability towards both organisms. The decrease of bacteria was observed to increase with the increase in chitosan content [14]. Also, some natural chemicals, such as cyclodextrins, promise to create long-lasting antimicrobial textile finishes; these cyclic oligosaccharides are characterized by an exterior hydrophilic surface and an interior lipophilic chamber [15]. In recent years, the textile industry has seen an uptick in using cyclodextrin and its derivatives [16]. Another no-metallic coating agent is triclosan, and its lipophilicity makes it very hydrophobic to water, ethanol or diethyl ethers are examples of soluble solvents [17]. Triclosan is effective because it blocks the microbe's ability to synthesize lipids by blocking the surface of the enoyl-acyl carrier protein reductase enzyme, which is needed for fatty acid synthesis and is required for the construction of cell membranes and lipid biosynthesis [18]. This is one of the reasons why it is utilized as an anti-fungal agent in the textile industry. But when bacteria assemble, they produce biofilm, and biofilm is a bacterial population with an extracellular matrix composed of proteins, polysaccharides, and DNA, infections that entail biofilm production are persistent and challenging to cure [21]. Using metal oxides as an alternate therapeutic technique might be a better option than other no metallic coatings agents. To prevent microorganisms' growth due to antibiotic resistance evolution[19]. The metal ions' ability to kill bacteria may be tied in some way to their affinity for connecting to specific ligand atoms found in biomolecules and other biological components [20].

1.2.4. Nanometal-Coated Cotton Composites

Metallic materials have been the subject of extensive study because of their broad range of potential uses; their particle size distribution, form, structure, microstructure, composition, and uniformity are all important elements to consider when researchers have taken an interest in metals [21]. Nanoparticles of metal oxide like silver (Ag NPs), titanium (Ti NPs), and zinc oxide (ZnO NPs) coating with cotton innovative, antimicrobial properties based. Titanium alloys have been utilized to build a wide range of implantation and fixation devices due to titanium's biocompatibility and inert properties within the medical field [22]. Furthermore, it turns out, TiO_2 is a rather good antibacterial substance. Antifungal and antibacterial were demonstrated in a prior investigation. And moreover Nano-TiO_2 has a photocatalytic effect, and when exposed

to light, photons with energy equal to or greater than the band gap of the titanium dioxide excite electrons up to the conduction band, resulting in a reduction of the bacterial count in the treated cotton fabric sample compared to the untreated cotton fabric sample with both Staphylococcus aureus and Klebsiella pneumonia. Free-radical oxygen is produced when excited electrons in the crystal lattice combine with atmospheric oxygen as a result of oxidation-reduction events, these oxygen atoms are capable of destroying the microbial cell wall [26]. Then another metal that has been explored is widely used because of its antibacterial properties. As a barrier against bacteria and other waterborne pathogens in water filter membranes, thanks to their time-delayed releasing qualities, the Ag NPs [27]. AgNPs, when administered to a tissue, were found to possess antibacterial and cytotoxic characteristics; the Ag NPs displayed a robust antibacterial impact on both Gram-positive and Gram-negative bacteria while also exhibiting minimal cytotoxicity; the antibacterial effect was detectable even after ten washes of the sample [23]. Ag NPs quickly connect with microorganisms' membranes to combat or prevent infectious diseases, resulting in cell death [24]. Another metal ion used as an induction for cotton is zinc oxide (ZnO NPs), zinc (Zn) is the highest abundant element on earth, and Zn is a micronutrient that is necessary for the survival of all living things [25]. It is necessary for the functioning of enzymes belonging to six distinct groups [26]. Clinical evaluations were carried out under two situations: 21 patients utilized medical textiles with ZnO NPs coated on them and another 16 patients employed medical textiles without coating. According to the findings, patients wearing modified fabrics are less likely to be infected with nosocomial pathogens. The modified textiles showed nontoxicity compared to the uncoated NPs material [27]. Nanomaterials made of zinc oxide have several desirable qualities, including remarkable mechanical and strength characteristics and antistatic, antibacterial, and UV-absorbing attributes [28]. Antibacterial fibres have been developed to help prevent the spread of bacteria and diseases by clothing. This has resulted from a greater focus on personal hygiene, the transfer of diseases through touch, and the need for additional layers of defence [29]. Studies have been conducted on the effects of metal-based NPs on textiles due to their potent antibacterial qualities but not all metal ions have received this attention towards the coating on the fabric; this is the case of Lanthanum (La), Cobalt (Co), Gallium (Ga). In the last few decades, the fields of nanotechnology have known an essential growth in the industrial areas

and, lastly, in medical fields, the presentation of a nanomaterial as an antibacterial agent has a particular recognition thanks to its physical-chemical capacity primarily due to the surface/volume size ratio, after examination the authors reported that the toxicity of Lanthanum oxide against gram-positive *staphylococcus aureus* but not against *Escherichia coli* and *pseudomonas aeruginosa*, they speculated that the lanthanum oxide produced this effect by interacting with gram-positive bacterial cell wall [30]. Another antibacterial is Ga, a semi-metallic element with three valences that has demonstrated antibacterial action against various significant human diseases. It is believed that its replacement in critical iron-dependent processes of bacteria is responsible for this antibacterial effect [31]. Another solution to eliminate bacteria can also be through cobalt ions. The antibacterial capabilities of the synthesized cobalt oxide nanoparticles showed a considerable reduction in the colony formation of gram-positive and gram-negative bacteria that were investigated. In line with the findings of this investigation, earlier research has demonstrated that cobalt oxide nanoparticles, either on their own or in combination with other substances, had antibacterial properties [32, 33].

1.3. PROBLEM STATEMENT

Cotton fabric is among the most popular materials in the world and has been produced and used since antiquity. It is an affordable and durable natural fibre for textiles. This plant-based fibre may retain heat because of its porous structure, which allows it to absorb more than 8.5% of its weight in water [34]. Cotton's absorbent characteristics make it necessary for sanitizing or cleaning, although using various hydrophilic cotton products to treat it. The fact that commercially available cotton has undergone processes like carding and chemical treatments like bleaching and others to eliminate the fibres' resinous and fatty components, making them extraordinarily absorbent, but it is time-consuming, and the result and the cotton produced can still be 100% non-sterile. It looks like a good idea to provide them with an antimicrobial barrier function delivered by an active substance to protect them from bacteria. To achieve this objective, the active compounds that are utilized inhibit the growth of germs and, as a consequence, lessen the detrimental impacts that these germs have, their proliferation and, as a secondary effect, a reduction in the crash that bacteria have as a direct result

of their action. The lack of newly developed antibiotics on the market has increased the urgency of the need for preventative measures to be taken against an impending crisis in global health. In this way, antibacterial coatings have become a bustling area of research and development, which the increasing urgency has actively urged to find alternatives to conventional antibiotics.

1.4. OBJECTIVE OF THE THESIS

Generally, the main objectives of this research project are to investigate and evaluate the microstructural, antibacterial, and biological properties of Nanometal (Ag, La, or Ga)-Cotton fabric composites.

Here the aim of this thesis can be summarized as,

- To synthesize and characterize Nanometal (Ag, La, or Ga)-Cotton fabric composites using co precipitation method and to characterize the abovementioned materials utilizing XRD, FTIR, SEM and TGA techniques.
- To evaluate the antibacterial properties of Nanometal (Ag, La, or Ga)-Cotton fabric composites against Staphylococcus aureus bacteria.
- To study the cytotoxicity behavior of the prepared materials when cultured with a mouse fibroblast cell line for 24 hours using deep blue assay.

1.5. SIGNIFICANCE OF THE THESIS

Incorporating new functionalities using nanometals like La, Co, or Ga carries a bactericidal and fungicidal action. Their application of these nanoparticles to the cotton industry may be brought about new possibilities of uses for traditional materials, and the finding of this study will help produce more coating elements in medical applications. Incorporating nanomaterials into porous substrates like textiles typically requires a series of steps, the use of expensive reagents and procedures, significant amounts of energy, and the production of a considerable amount of effluents that need to be treated, therefore to enable the manufacturing of these materials on a broad scale,

it is crucial to create new methods that are both easier to carry out and have lower overall operating costs.

PART 2

LITERATURE REVIEW

2.1. NANOPARTICLES AS ANTIBACTERIAL AGENT

In light of the growing concerns over bacterial strains resistant to antibiotics and infections connected with biofilms, there is a need for antibacterial treatments that are effective over the long term and for preventative treatments of biofilms [35]. As a result of the widespread usage of metals throughout human history, metals, in fact, have a long account of use in medicine, particularly in the field of antimicrobial therapy they were constructed about 1125 B.C astringents made from copper salts were employed by the Egyptians [36]. Copper and silver were both utilized by the Indians, Egyptians, Persian rulers, Phoenicians, Greeks, and Romans to preserve food and sterilize water, respectively [36]. Later, silver was utilized as suture material and an infection-prevention agent. Throughout history, different applications have used the antibacterial qualities of metals; however, since the discovery of antibiotics in 1920, the antimicrobial properties of metals in medical applications have drastically decreased [37]. But in the face of growing concerns about resistant bacterial strains and biofilm-associated infections associated with biofilms metals are once more the answer to the problem of fighting microorganisms.

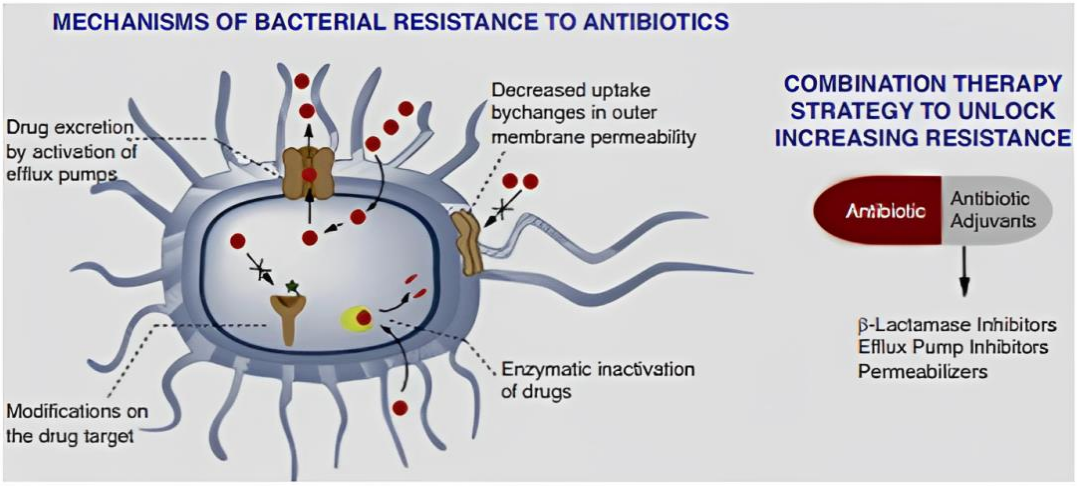

Figure 2.1. Mechanisms of bacterial resistance to antibiotics [32].

Nanoparticle metals such as Ag, copper (Cu), gold (Au), titanium (Ti), and Zn, each with their own unique characteristics, potencies, and activity spectra, they have been recognized to possess antibacterial activity for ages. This knowledge has been put to use in various applications. In recent years, nanotechnology has made available a wealth of prospects across a variety of scientific and technological domains, because of their potential antibacterial effects, several different kinds of nanoparticles and their derivatives have garnered a lot of attention recently [33,34].

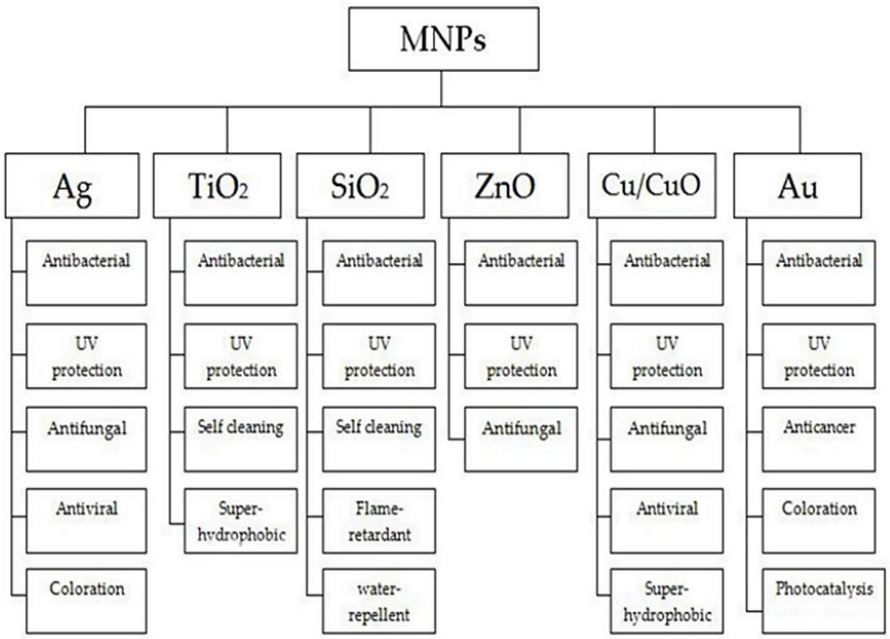

Figure 2.2. Metal nanoparticles and their functions [41].

Metal atoms tend to bind to the thiol group of enzymes, inhibiting the enzymes' ability to perform their function. It has also been hypothesized that metal ions can bind between pyrimidine and purine base pairs, thereby breaking the hydrogen bonds that hold the two antiparallel strands of DNA together and causing the DNA molecule to be destroyed. However, this needs further research [42, 43]. It has been shown that the dimensions of the metal nanoparticles have a significant impact on their antibacterial activity [44]. Antimicrobial action is correlated with shape in several ways NPs interactions with periplasmic enzymes can result in variable degrees of bacterial cell damage [45]. Research has demonstrated that the zeta potential of NPs significantly impacts the adherence of bacteria to the particles. This is because of the electrostatic interaction between the positively charged nanoparticles and the negatively charged bacterial cell membrane. Because the nanoparticles have a positive surface charge, they will likely adsorb onto the bacteria's surface and are also tightly linked to the bacterium [46, 47]. The factors that influence antibacterial activity suggested are the production of reactive oxygen species (ROS), second the process of ion release, and third the interaction of NPs with the cell membrane, metal ions on the nanoscale scale are what make up the first stage of the antibacterial process, these ions enter the cell through a transmembrane protein, the size of the particle determines the entire process and it begins with the binding of the particle to bacterial cells, this results in the production of structural changes in the cell membrane as well as the blocking of transport channels [48]. Also, smaller NPs are more effective, but larger NPs have a higher absolute surface area, which allows for a better adhesion property thanks to the Van der Waals force; if the NPs are internalized, they can cause ionization within the cell as well as damage the intracellular structures, which ultimately results in cell death [49]. The ability of metallic nanoparticles to generate reactive oxidizing species (ROS) is crucial to their success as antibacterial agents. The reactive oxygen species are made up of short-lived oxidants like superoxide radicals (O_2^-), hydrogen peroxide (H_2O_2), hydroxyl radicals ($^{\bullet}OH$) and singlet oxygen ($^1(O_2)$) because of the high level of reactivity of these species, reactive oxygen species (ROS) are capable of disrupting peptidoglycan as well as cell membranes, deoxyribonucleic acid (DNA), messenger ribonucleic acid (mRNA), ribosomes, and proteins ROS can impede not only transcription but also translation, as well as enzyme activity and the electron transport

chain. In order to exert their harmful effects, many metal oxide nanoparticles rely primarily on producing reactive oxygen species [50, 51].

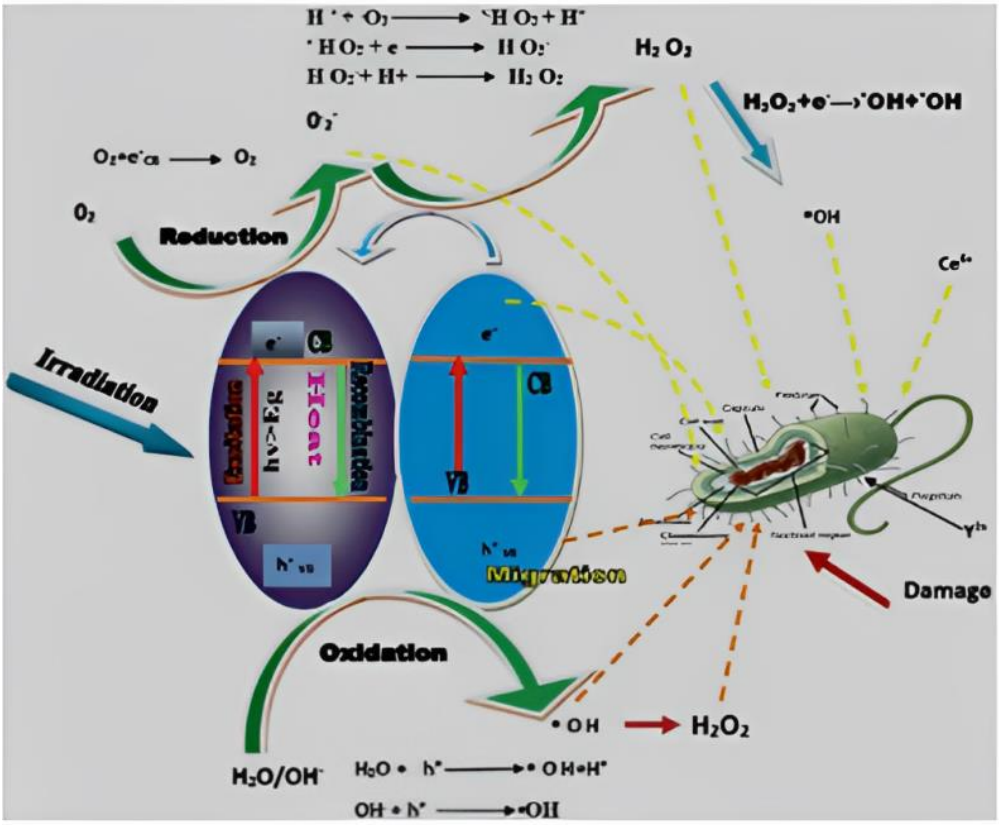

Figure 2.3. The action of reactive oxygen species on bacteria [52].

2.2. LANTHANUM

2.2.1. The Physical property of Lanthanum

Chemical, metallurgical, and physical properties of rare earth elements(REEs) are determined by their electronic structure; there are four possible oxidation states for REEs: trivalent for all of them, tetravalent for Cerium (Ce), Praseodymium (Pr), and Terbium (Tb), and divalent for Samarium (Sm), Europium (Eu), and Yttrium (Y) because 4f electrons are part of the ion core and do not directly engage in bonding with other elements, the lanthanides are chemically very similar and difficult to separate from one another Valence electrons are 5d6s2 for all 14 lanthanides, 3d4s2 for Sc, and 4d5s2 for Y [53]. The ionic radius of lanthanides decreases as molecular weight

increases from La to Lutetium (Lu), a property known as lanthanide contraction, some elements namely those in their divalent and tetravalent forms are an exception to this rule since the 4f orbital is no longer insulated from the growing nuclear charge, the 5s and 5p orbitals have penetrated it causing the contraction, as the atomic number grows the ionic radius decreases due to the increased attraction of the positively charged nucleus to the electrons tugging them in the absence of adequate shielding since density, melting temperature and hardness often increase from low to high molecular weight across the series, while basicity normally declines, the contraction is essentially what makes separation of the lanthanides practically practicable, in particular, the fundamental nature provides the groundwork for a variety of separation methods [54]

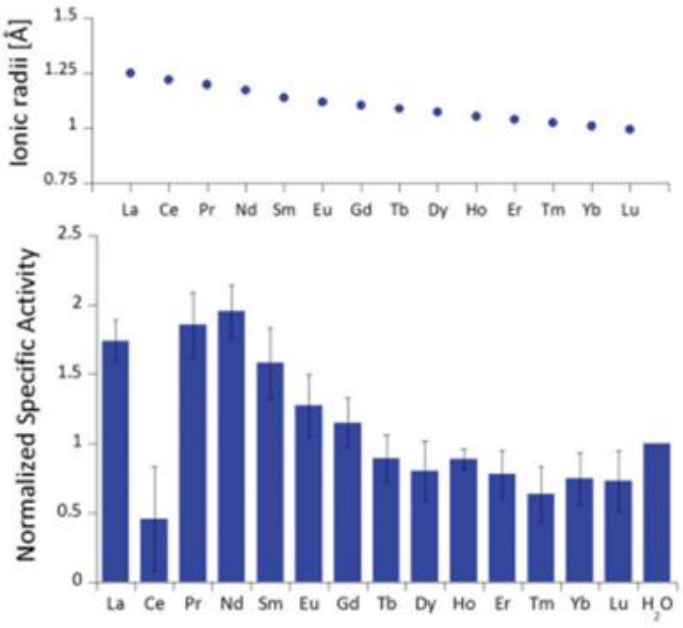

Figure 2.4. The ionic radii of lanthanide [47].

Despite the numerous chemical similarities amongst the lanthanides, their physical characteristics differ a lot, their plots of elemental melting temperatures versus molecular weight.

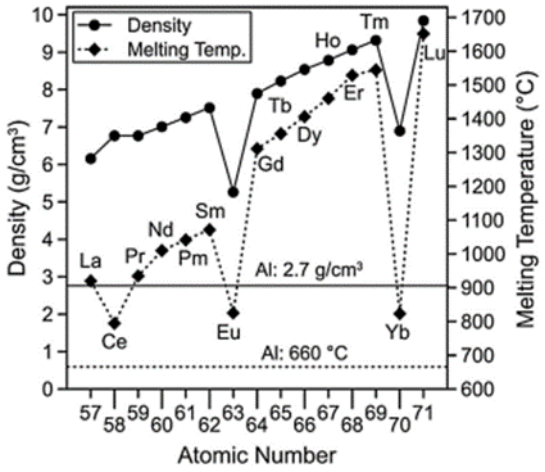

Figure 2.5. Rare earth melting and transition points [56].

In the field of biomedical research, lanthanide complexes are utilized as contrast agents for MRI scans in conjunction with their Luminescent properties, the luminescence of lanthanides appears linked to the energy levels of Ln(III) ions relative to their 4f orbitals due to the repulsion between electrons in the orbitals caused by coulombic interactions, the electronic configuration is first separated into terms, spin-orbit coupling then separates the terms into discrete J levels the spin multiplicity represented by 2S+1, the total orbital angular momentum represented by L and the kinetic momentum represented by J make up the different levels of the free ion and are symbolized by the symbols S, L, and J, respectively [48]. Because the filled 5s and 5p orbitals shield the 4f orbitals, the resulting J energy levels are sharply defined, and the transitions between them are obvious, resulting in distinct emissions bands for each lanthanide.

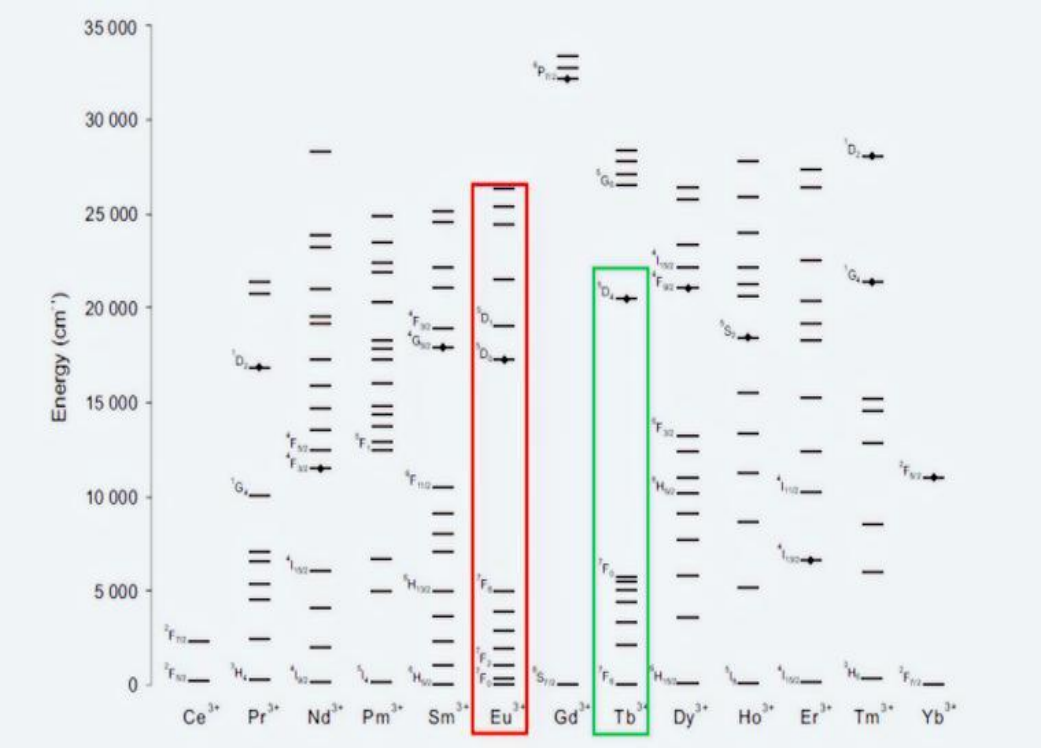

Figure 2.6. Energy diagram of lanthanide ions in aqueous solution [57].

For lanthanide ions in a coordination setting, the electric field of the matrix allows for additional sub-division of the J levels [49]. There are two types of radiative transitions that lead to the absorption and subsequent emission of light: magnetic dipolar transitions with permitted parity and electric dipolar transitions with prohibited parity [50]. The luminescence of lanthanides is visible in a wide spectral range, which extends from the ultraviolet to the infrared. It demonstrates a wide Stokes displacement and the emission lines it produces are very thin because it is unable to have transitions for the first two elements (there are no electrons in the f orbital for lanthanum (III), and the orbital is saturated for lutetium (III)), lanthanum, lutetium, and prometheum do not have luminescence properties, this is because pmetheium (III) is both radioactive and unstable [49].

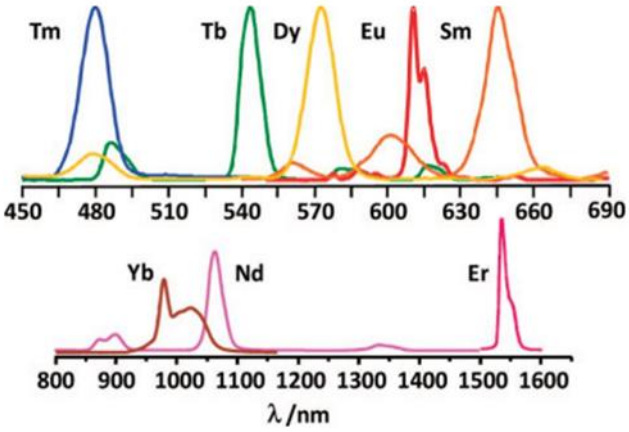

Figure 2.7. The emission spectrum of some lanthanide [58].

2.2.2. Antibacterial Activity of Lanthanum

As a new approach for combating emerging infections using lanthanide ion and the NITph-p-Cl radical (nitronyl nitroxide) in conjunction with the hexafluoro acetylacetonate (HVAC) ligand, Zhang et al. reported the existence of four different lanthanide complexes. Ln (HVAC)3(NITph-p-Cl) metals Er, Tb, Dy, and Gd were used to synthesize two different types of complexes. The antibacterial activity of these complexes was evaluated against a broad range of bacterial species. According to the study, all Ln complexes were shown to have more antibacterial activity than lanthanide ions or radicals[60]. The results of the antibacterial testing demonstrated that when compared to the other three Ln complexes, the Gd complex had the highest antibacterial activity against Escherichia coli, the antibacterial activity of the other three complexes made up of Er, Tb, and Dy against *Escherichia coli* was reported to be less than that of Gd, due to its superior antibacterial capability, the Gd complex can be employed in a wide range of settings [61]. Trivalent La, Gd, Nd, Pr, Er, Sm, Tb, and Dy metal complexes with the Schiff base ligand (N,N-bis(1-naphthaldimine)) were produced by [62] from 2-hydroxy-1-naphthaldehyde and o-phenylene diamine to facilitate interaction with the central metal, the ligand features two phenolic oxygen atoms and two imine nitrogen atoms ligand and its Ln(III) complexes demonstrated ordinary antibacterial efficacy against *p. aeruginosa* and *E. coli* based on their biological properties it was found that all lanthanide complexes containing the (N,N-bis(1-naphthaldimine) ligand had superior antibacterial activity against gram-positive

bacteria but weak action against gram-negative bacteria [63]. As a ligand [64] produced binary complexes of trivalent La, Sm, Gd, and Dy employing FCA (Furan-2-carboxylic acid), some gram-negative and gram-positive bacterial species were used to assess the complex's antibacterial and antifungal properties compared to the parent ligand, manufactured complexes had much higher inhibitory action against certain bacteria and fungi in the antibacterial and antifungal investigation antifungal activity against Aspergillus niger, Aspergillus fumigatus, and Aspergillus flavus, as well as antibacterial activity against *Escherichia coli* (gram negative) and *Staphylococcus aureus* (gram-positive) it shown in studies of the binary complexes of La, Sm, Gd, and Dy with FCA ligand synthesized Eu(tfn)3(phenedione), Eu(hft)3(phenedione), and Yb(hfa)3(phenedione) complexes by reacting Eu(tfn)32H_2O, Eu(hft)32H_2O, and Yb(hfa)32H_2O molecules with phenedione accordingly. The antibacterial study confirmed the potent antibacterial activity of phendione and its lanthanide complexes with the highest antibacterial activity revealed against *Proteus penneri* bacteria compared to *Escherichia coli* and *Staphylococcus aureus*, PL spectra (Photo Luminescence spectra) and other spectral techniques were used to characterize the structural properties of the complexes [64, 65]. Most of Ln complexes revealed the antimicrobial activity of some bacteria complexes of La and Pr were found to be more active against *P. aeruginosa* than the standard antibiotics like cephalexin and cephradine; the gram-positive bacteria were much more sensitive than the gram-negative bacteria towards the Ln complexes trivalent lanthanide metals with Schiff base ligand was derived from 2-hydroxy-1-naphthaldehyde with o-phenylenediamine [66]. Therefore, it was proven beyond a shadow of a doubt that these complexes inhibited bacterial growth against gram-positive bacteria. At the same time, the ligand showed better antibacterial activity than its complexes against *Escherichia coli*. This means that the complexes of lanthanide metals with TC ligand exhibited less antimicrobial properties than the parent ligand against gram-negative bacteria (*Escherichia coli*) but more against gram-positive bacteria [67]. The biological investigation of trivalent a series of lanthanide salts using chloride and nitrate salts of n-salicylideneamino)-3-carboxyethyl-4,5,6,7-tetrahydro benzo[b]thiophene (HSAT) has been developed by[66], the biological properties of these two different series of new complexes involving coordination number 12 were investigated. Six complexes each of La, Nd, and Sm were chosen for the biological test from a total of twenty

different complexes containing the elements La, Pr, Nd, Sm, Eu, Gd, Dy, Tm, and Lu, after testing the ligand and its six selected complexes for their antibacterial and antifungal activities against several harmful bacterial and fungal species, it was determined that the ligand possessed physiological activity. In contrast, the complexes extended the biological activities of the ligand, and It was discovered that complexes containing La, Nd, and Sm have antibacterial and antifungal effects that were superior to those of ligands against some species of harmful bacteria and fungi [66]. Coordination with various chelators or ligand systems demonstrating possible biological characteristics makes metal complexes of lanthanides desirable. The synthesis of prospective biologically relevant compounds has thus far centred mostly on modifying and enhancing Ln family members.

2.3. COBALT

2.3.1. The Physical Property of Cobalt

Although it wasn't discovered until 1735 by the Swiss scientist Georg Brandt, cobalt has been used for thousands of years to colour glass, ceramics, and valuable stones (cobalt blue) by ancient Egyptians, Persians, and Chinese cultures, first identified as an element in its metallic form in 1780 by Torbern Bergman due to its toxicity and the fact that its presence contaminates components that require a high level of purity in their extractions. Hence, the name Kobalt comes from the German word kobold, which means evil spirit, it wasn't until the 20th century that it started being made, and even then, it was mostly a waste product from the mining of nickel, copper, and arsenides [68]. Cobalt is a naturally occurring element with the atomic number 27, and its occurrence in the earth's crust is 0.002%, which translates to 20 parts per million. This places it as the 33rd most prevalent element on the planet. On the periodic table, it can be found in the 9th period of the d valence block, which is typical of transition metals. Its primary valences are +2 and +3, and its density is 8.9 $g.cm^{-3}$; its melting point is 1450 degrees Celsius, while its boiling point is 2900 degrees Celsius. In addition to being located in plants, animals, and meteorites, it is also possible to discover it in the earth's soil, rocks, and seas [69]. Crystalline structures of the body-centred hexagonal

type, also known as the shape, are the allotropic forms of cobalt with the highest degree of structural stability [70].

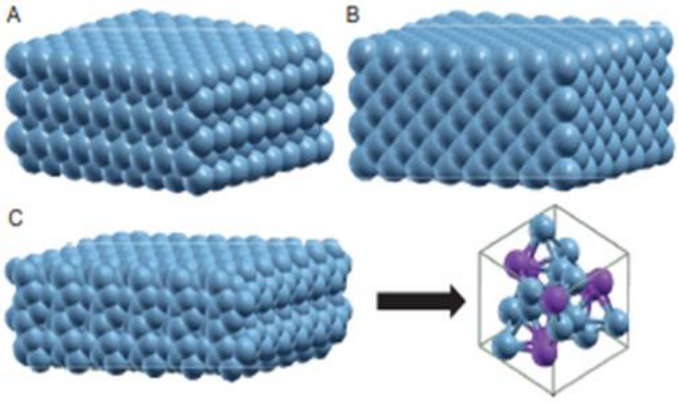

Figure 2.8. Cubic structure of cobalt [71].

When subjected to heat treatment at temperatures as high as 417 degrees Celsius, this structure transforms into a cubic face crystal structure centered (CFC), which can be stabilized by adding a negligible quantity of iron [70]. Due to the high degree of homology between the properties of cobalt and those of the element iron, cobalt is categorized as ferrous metal, it is a ferromagnetic element that is extremely strong and hard, and it has magnetic properties that are comparable to those of iron, a result of its compatibility with this component, possesses features of a siderophile in addition to this, according to Goldschmid's geochemical classification it is an element chalcophile because of its affinity with the element copper [72]. Cobalt uses have changed over the years before the rise of high-tech industries, the metal was primarily used in alloys, superalloys and catalysts but not batteries, Computers, phones, and electric cars boosted the use of cobalt in batteries cobalt's composition varies in batteries, Lithium cobalt oxide ($LiCoO_3$) ion batteries contain more than 60% cobalt, while lithium nickel cobalt aluminum oxides (Li-Ni-Al-Co) batteries comprise 9%, above 15% cobalt is in nickel metal (Ni-MH) batteries, nickel–cadmium (Ni-Cd) batteries contain 1 to 5% of cobalt hydroxides as a catalyst, it is used in the polymerization and oxidation stages of plastics to manufacture resins and hydrotreatment reactions, transformation of natural gas into diesel octane, and many other processes, it is also used in dental applications, prostheses, and low-energy Al-Ni-Co magnets, other applications involve functions as a binder material in high hardness such as cemented carbides and diamond composite

tools, as a pigment for the creation of glass, enamels, and ceramics and as an ingredient in electronic connectors and integrated circuits [69].

2.3.2. Antibacterial Activity of Cobalt

The element cobalt (Co) is of fundamental importance in medicine because this metal is present in some enzymes and is a component of vitamin B12 in the form of Co (III). Being present in the center of its structure, this vitamin participates in several critical biochemical processes such as the synthesis of amino acids and nucleic acids and in the development of erythrocytes, also used in radiotherapy the radiation ionizing (rays) released by cobalt-60 to target [73].

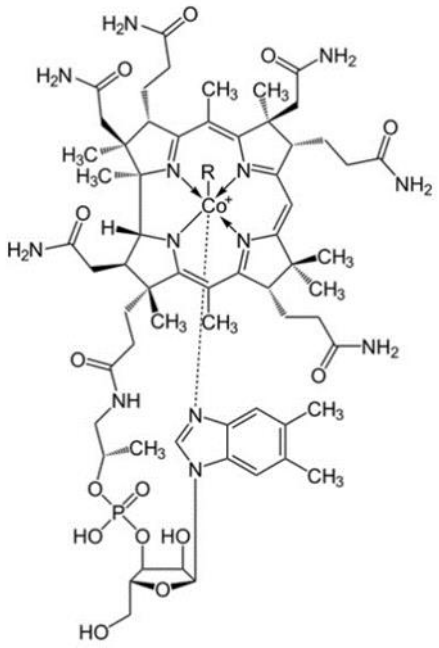

Figure 2.9. Cobalt vitamine b12 [74].

Several studies demonstrate the usefulness of compounds containing cobalt (III), metal complexes of Co (III) were shown to have an inhibitory effect on the enzyme urease, which is present in a wide variety of species, including plants, algae, fungi, and bacteria, this effect was demonstrated [75]. Conducted studies with free sparfloxacin and coordinated to the metallic ion Co^{2+} and proved that the complexed antibiotic increases the efficiency of the drug against bacteria; Staphylococcus aureus, Salmonella typhi, Escherichia coli and Bacillus subtilis [76]. Cobalt alloys offer a

great combination between biocompatibility, mechanical strength and corrosion resistance; as a result of which, it is suitable for use in the production of artificial joint materials it was also recently revealed that in addition to causing a hypoxic response, Co^{2+} incorporation might also improve the antibacterial activity of titanium-based bone implants, this finding provided evidence that Co^{2+} had an additional effect as an antimicrobial agent [77]. Direct binding of Co^{2+} to bacterial DNA generates reactive oxygen species (ROS), which can trigger many pathways leading to the death of bacterial cells. Reactive oxygen species (ROS) include peroxides and other reduction products of oxygen that play a significant role in DNA and cellular damage, including the destruction of bacterial cell membranes [78, 79]. Many potentially fatal diseases can be traced back to bacteria, making this a pressing global concern; antibiotic-resistant bacteria are particularly worrisome bacterial infections cause significant morbidity and mortality annually, highlighting the need for better international infection control measures so the antimicrobial and cytotoxic effects of cobalt-based nanoparticles (CBNPs) have been shown against several microbial species. These effects seem to be dose-dependent [80, 81]. In the illustration, the authors presented the biogenic synthesis of Cobalt nanoparticles utilizing Hibiscus cannabinus leaf extract and established their antibacterial effectiveness against Bacillus subsites and Escherichia coli [82]. When tested on Gram-negative and Gram-positive bacteria, the Co_3O_4 NPs actively inhibited Klebsiella pneumonia and Bacillus lichenicolous. The low-concentrated Co NPs is non-toxic in vivo, making them a viable alternative as a novel antibiotic, and a study shows that Co NPs have more excellent antibacterial activity than the traditional antibiotic medication ciprofloxacin [83]. For antibacterial purposes, cobalt nanoparticles have shown promise against a wide range of microorganisms, and Co NPs have also demonstrated significant antibacterial activity against multidrug-resistant species such as Staphylococcus aureus, Proteus spp, Bacillus subsites, and E. coli [77]. CoFe2O4 nanoparticles were shown to have the ability to adhere to negatively charged bacterial cells and to be effective against Gram-negative bacteria at lower doses, as demonstrated by their work [84, 85].

Nonetheless, NPs' ability to detect bacteria was sensitive to variables such as bacterial strain, concentration, and particle size. Under laboratory conditions for bacterial systems, for instance, small Co NPs demonstrated statistically higher toxicity than

larger Co NPs90 [86]. The surfaces of the Co NPs can come into contact directly with the bacterial outer membrane, and this can cause the membrane to become damaged, which in turn destroys the functions and growth of the bacterium. In addition to this, the small Co NPs that have a high surface-to-volume ratio interact with the bacterium's outer membrane, which results in a change in the membrane's permeability. Because of this increased permeability, the NPs and the medications contained within them canter the bacterium, where they can then kill the bacteria more efficiently [87, 88].

2.4. GALLIUM

2.4.1. The Physical Property of Gallium

On the periodic chart, the element gallium may be found in group IIIA at the atomic number 31 Paul-Émile Lecoq de Boisbaudran in France is credited with making the initial discovery of it would appear that the name of this metal was taken from the Latin word for France, which is "Gallia"[89]. As one of the few metals that are virtually liquid at room temperature and can melt when held in hand, it has a brilliant silver-white colour and a melting point of 28.7 °C. He is also one of the few metals with vivid colour. However, gallium does not serve any physiological purpose in the human body. The element's Specific properties make it possible to interact with biologically significant cellular processes and proteins, particularly those involved in iron metabolism. Because of this, various gallium compounds have been developed for use in medicine as diagnostic and therapeutic agents, particularly in treating metabolic bone disease, cancer and infectious disease [89]. The inorganic substance known as gallium oxide (Ga_2O_3) can be found in five distinct forms, or polymorphs (α, β, γ, δ, e, ε); the α -Ga_2O_3 phase is the phase that has the highest thermodynamic stability, the other stages show 24 metastable states under ambient conditions and transform into β-Ga_2O_3 at temperatures above 600°C [90].

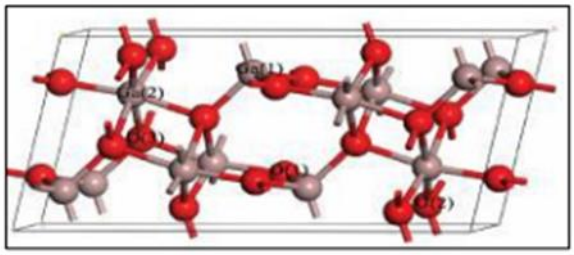

Figure 2.10. A monoclinic crystalline structure of β-Ga2O3 [80].

Gallium is a metallic trace element found in coal, bauxite, and other minerals. It is virtually liquid at ambient temperature. It expands in solid state and has a wide range of applications. It is a crucial ingredient in many low-melting-point alloys and finds application in semiconductor technology. The gallium (III) (Ga^{3+}) ion, which predominates in trivalent compounds, is acidic and strongly binds to strong Lewis bases like hydroxyl (OH^-) cation $[Ga(H_2O)_6]^{3+}$ can act as a proton donor, giving $[Ga(H_2O)_5(OH)]^{2+}$ $[Ga(H_2O)_4(OH)]^+$, the deprotonation of mononuclear species causes hydroxide precipitation, which in turn causes the pH (hydrogen ion potential) to rise to allow for the eventual production of $[Ga(OH)_4]$. Thus, two gallium ions are available for use in metabolic biochemical reactions, $[Ga\ (H_2O)_5(OH)]^{2+}$ in a medium with a weak acidic pH and $[Ga\ (OH)_4]$ in solutions ranging from neutral to a weak alkaline pH [91]. Ga (III) is thought to be similar to Fe (III) (69.0 pm) and Al (III) (67.5 pm), especially when combined with phosphorus, due to its ionic radius of 61 pm in tetrahedral coordination and 76 pm in octahedral coordination, specifically when paired with phosphorous, phosphates are among the most stable chemicals. Gallium has such a strong affinity for phosphorus that gallium phosphates are among them [91].

2.4.2. Antibacterial Activity of Gallium

The similarities between gallium and iron's metabolic characteristics are the primary source of the clinical interest in this element, both elements exhibit nearly identical chelate and protein binding abilities, and their ionic radii are very similar to one another since transferrin and lactoferrin. The two most prominent transporters of iron do not discriminate between gallium and iron, all gallium in the blood is present in the plasma as complexes with these proteins [92]. According to [93], the ionic radius of gallium (III) is comparable to that of iron (III), which means that the two elements

have some features, Ga^{3+} has an octahedral ionic radius of 0.620 Angstrom, whereas Fe^{3+} has an octahedral ionic radius of 0.645 at high speed, in comparison, the tetrahedral ionic radius of Ga^{3+} is 0.47, while the tetrahedral ionic radius of Fe^{3+} is 0.49 [93]. Now, gallium has been added to a bioactive material only in ionic form, such as bioactive glass [94]. Or in calcium phosphates [95]. Over the past few years, active nanostructured metals have found a new antibacterial application pathway due to nanotechnology advancements[96]. Following this, there is an increase in the cellular uptake of ions due to the subsequent release of ionic species within cells caused by the dissolution of nanoparticles. This process is frequently referred to as "the Trojan horse mechanism". The high intracellular concentration that was achieved due to the breakdown of nanoparticles inside the cell most likely causes a significant amount of oxidative stress.

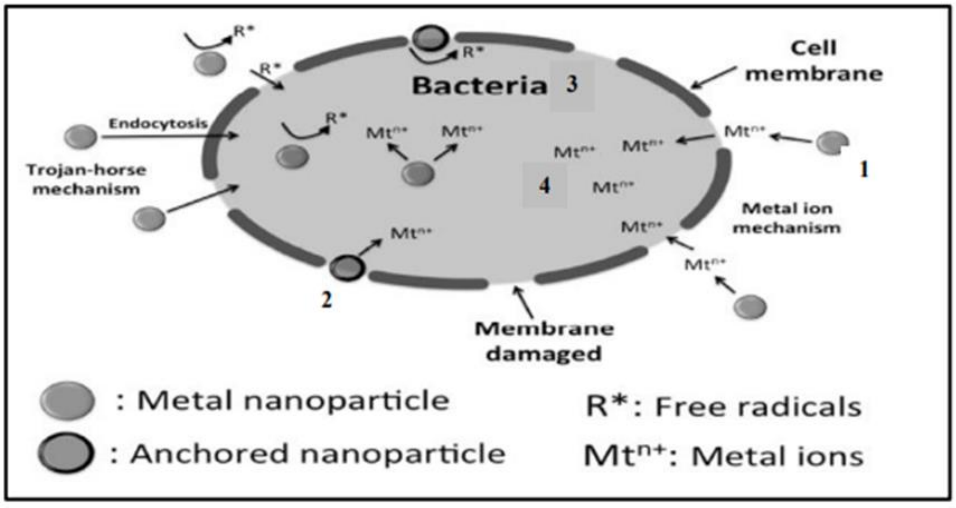

Figure 2.11. Oxidative stress action [97].

Metals are distinguished by their ability to take part in redox processes, which define their propensity to accept electrons from a donor [87]. If the levels of these species surpass the capacity of the cell's antioxidant defences, they can cause oxidative stress, which can damage the cell's DNA, proteins, and lipids [88,89]. Furthermore, increased in intracellular ROS promotes inflammatory processes that can cause the cell to undergo apoptosis (programmed cell death [90]. Therefore, partially reduced forms of molecular oxygen (O_2), such as hydrogen peroxide (H_2O_2) and superoxide ($O^{2\bullet-}$), are generated during the hazardous process of aerobic respiration. In the presence of

certain metals, the Fenton reaction, mentioned in, takes place, this reaction is characterized by an increase in the toxicity of oxygen, a catalyzed transfer of electrons from a donor biomolecule to H_2O_2, and the production of highly reactive hydroxide (OH) and radical hydroxyl (OH^-). The presence of ROS is the foundation for the majority of the processes that attempt to account for the activity of metal biocides [91]. These reactions, the molecule H2O2 is broken up in various ways to yield free radicals see Equality 2.1.

$$Fe^{2+} + H_2O_2 \rightarrow Fe^{3+} + OH^- + OH \quad (2.1)\ [91]$$

External metals can increase the process, causing extra ROS compounds and oxidative stress in the cell. Using gallium nanoparticles instead of ions can lead to an advanced, controlled, prolonged local antibacterial action [103]. Several medical uses have been discovered for gallium in its ionic state (3+), including its ability to diagnose cancers, treat hypercalcemia, limit bone resorption, have anticarcinogenic properties, and fight bacteria [93]. The ability of Ga^{3+} to mimic Fe^{3+} is primarily responsible for the wide spectrum of pharmacological action that gallium possesses. This is primarily because the charge/radius ratio of the two ions is almost identical. In general, it is possible to say that the broad spectrum of pharmacological action that gallium possesses is due to the ability of Ga^{3+} to mimic $Fe^{3+,}$ as a result, most biological systems cannot distinguish between Fe3+ and Ga3+. However, Fe^{3+} is reduced under physiological conditions, Ga^{3+} is not. Therefore, it cannot participate in the key iron-dependent activities that make life possible. Most microbes cannot grow without the Fe3+ ion, which is important for numerous metabolic processes and DNA synthesis (Deoxyribonucleic Acid) Ga^{3+} is able to bind to the locations on transferrin where Fe^{3+} is located. Certain bacteria can acquire it from transferrin, and mononuclear phagocytes at the sites of inflammation can integrate it [104]. In order to live and reproduce, most organisms require the iron ion (Fe^{3+}) pathogens, hence offering a possible focus for preventative measures and therapeutics. Incorporating nitrate of gallium into culture media containing *Mycobacterium spp* has proven in vitro that gallium has the ability to suppress the growth of intracellular bacteria by interfering with iron metabolism [105]. An alternative approach uses the Ga transition metal to disrupter the bacterial iron metabolism [106]. In contrast to $Fe^{3+,}$ Ga^{3+} cannot be reduced, making it a potential

inhibitor of Fe-dependent activities, many of iron's biological roles depend on the successive oxidation and reduction of $Fe^{3+,}$ gallium inhibits DNA synthesis and causes changes in its three-dimensional structure, exerts a modulating effect on protein synthesis and inhibits the activity of enzymes such as DNA polymerases and ribonucleotide reductase, gallium alters membrane permeability and functions mitochondrial, gallium has been shown to have antiproliferative properties by inhibiting ribonucleoside diphosphate reductase (RDR), an enzyme necessary for the creation of DNA by facilitating the conversion of ribonucleotides to deoxyribonucleotides, R1 and R2 are two sub-units of the enzyme's overall structure substrate binding sites are located in the R1 subunit, while two ions Fe^{3+} connected by an oxygen bridge and a tyrosyl free radical are located in the R2 subunit, all of which are necessary for enzyme activity, by taking the place of Fe^{3+} in the RDR structure, Ga^{3+} inhibits enzyme activity by inducing a conformational shift [106]. Antimicrobial effects against iron-dependent bacteria have been attributed to trivalent gallium. Gallium (III) has recently been shown to be effective against Rhodococcus equi, an internal bacteria that causes pneumonia in foals [107]. Gallium was found to be successful in treating experimental syphilis in rabbits, killing *Mycobacterium TB* and *Mycobacterium avium*, and to prevent the development of malaria parasites, as detailed in an exhaustive review by [93]. According to the authors, gallium's capacity to enter microorganisms via its transport mechanisms iron certainly accounts for the activity; specifically, gallium's ability to disturb your iron metabolism and interfere with protein synthesis, the ability of gallium-bound transferrin to enter infected cells through the receptor of transferrin may be an advantage in the treatment of some intracellular infections, their bacterial infections are treatable with gallium nitrate, treatment of acne, boils, carbuncles, folliculitis, and other bacterial skin infections with a single topical application of a gallium nitrate solution was reported to be beneficial by [108], they also noted that two human ocular bacterial infections that were resistant to therapy were eradicated after a few hours of daily application of a 1% gallium nitrate isotonic ocular saline solution [108]. Gallium has been shown to kill both planktonic bacteria and biofilms in vitro and prevent the growth of Pseudomonas aeruginosa and biofilm production [104]. Although the effects of Gallium antibacterial have not been carefully investigated, they appear to be benign and even beneficial given that numerous enzymes containing iron are involved in the microbial metabolism of

infections; gallium can operate as a detrimental agent in these organisms, inhibiting or destroying cells by insertion into the composition of these protein networks [109]. Receptor-mediator endocytosis brings the iron gallium-transferrin complex inside the cell, where an oxidoreductase reduces it in the plasma membrane to release the iron ions bound to transferrin due to its lack of a 2^+ valence. Gallium is unable to follow the iron pathway farther into the cell. The sole plausible explanation is that polymorphonuclear leukocytes are able to replicate the conduction of the Fe^{2+} ion by forming the pentaaquahydroxy gallium ion $[Ga(H_2O)_5(OH)]^{2+}$, which formally has the same charge 2^+ as bivalent iron (Melnikov et al., 2008). All the gallium in the body is found in the plasma in the form of complexes with the two major iron transporters, transferrin and lactoferrin. According to Brittenham, under typical conditions, iron (III) occupies about a third of transferrin, leaving a huge number of empty sites for gallium (III) to achieve a significant amount of 2.7 mg/ml Ga^{2+} [110]. Gallium appears to be held by ferritins after it enters the cytoplasm of a cell, which are large proteins that display tissue-specific variation based on the mix of their subunits [111]. How gallium gets liberated from ferritin is poorly understood. However, plasma gallium attached to low molecular weight carrier molecules is interchangeable with physiologically inactive elements stored in ferritin and hemosiderin, thus, the two are in equilibrium [111]. Gallium's antibacterial potential has been the subject of some intriguing studies due to its propensity to inhibit iron uptake by specific microbes. Mycobacterium TB and Mycobacterium avium, both in the extracellular complex and inside human macrophages, rely on iron for their proliferation, and both gallium nitrate and transferrin-gallium have been demonstrated to impede this process gallium prevents Mycobacterium TB from acquiring iron within the phagosome of macrophages, leading to a bactericidal activity, which may be blocked an abundance of iron [105]. [112] Gallium deferoxamine B (Ga-DFOB) and gallium citrate are two gallium compounds that kill bacteria differently (Ga-Cit). Metabolomic analysis was used to delineate the effects of Ga-Cit on the bacterial cell. Exposure to gallium resulted in low concentrations of glutamate, an essential metabolite for P. aeruginosa and many amino acids, indicating that Ga affects various biosynthetic pathways. The antibacterial effect of Ga has been shown to vary depending on the carbon source, which has importance in the context of medical applications of gallium. According to [112], gallium have the potential to be used as an antibacterial medication against both

gram-positive and gram-negative bacteria[112]. Gallium nitrate is used clinically to treat hypercalcemia, and in vitro experiments with this salt have shown antibacterial and biofilm-preventing action against P. aeruginosa. Bacterial Fe^{3+} metabolism is inhibited by Ga^{3+}[113]. It is possible that the addition of nano-gallium as a new antibacterial component to a bioactive material such as hydroxyapatite (HAp), which is commonly utilized in bone/dental implant and engineering tissue, this would provide a composite with antimicrobial and tissue growth/repair promoting properties, making it ideal for use in wound care [114]. Because it is chemically similar to Fe (III), an essential element for the metabolism of pathogen cells, gallium (III) has proven useful as an anti-infective drug. This chemical element's anti-infectious and anti-inflammatory properties make it an attractive candidate for use in biomedical and other fields.

2.5. METHODS USED TO COAT NANOPARTICLES IN TEXTILE.

Due to their high surface area and capacity to hold moisture, textile fabrics, especially those created from natural fibres, are ideal for the growth of microbes. A wide variety of compounds have been used to make textiles antibacterial. There has been a significant uptick in interest from the academic and commercial sectors in creating new textile-based products based on immobilizing nano-phased materials [115]. The preparation and application of nanoparticle coatings onto cotton fibres have garnered much attention due to their promising applications. Currently, a wide range of nanoparticles (NPs) with varying structures can be immobilized onto the textile fibres in order to bring new properties to the textile product [115]. Cotton textile fibres and other substrates can be impregnated with metal oxide nanoparticles using sol-gel methods, co-precipitation, Sonochemical treatment, micelle method/reverse microemulsion, and Chemical Vapor Deposition are approaches that can be taken.

2.5.1. Sol Gel Methods

The sol-gel approach is the one that is employed at the moment to determine the functional qualities of the surfaces of textiles, and it is suggested that this method be used instead of others in the process of development, and the number of projects that

use it is growing each day. In recent years the sol-gel method has been shown to have functional properties (flammability, antibacterial protection, UV protection, and it has also been observed that it has begun to be used to provide anti-crease); these functional properties have been achieved by combining sols and gels [116]. Even multipurpose applications which allows for the provision of more than one functionality simultaneously are also available, and it employs a series of well-established traditional techniques. It is carried out in stages, these chemically dependent procedures may be completed in a single step using the sol-gel approach, and because it requires fewer of these potentially hazardous chemicals, the sol-gel method is also used for textile finishing [117]. This development holds a great deal of significance for the running of operations and shows promise for the conduct of future research. In addition, it implies increasing profitability while maintaining or improving the textile sector's quality [118]. In the sol-gel method, starting materials are metal alkoxides or metal sol is prepared using salts), solvents (alcohols) and catalysts [119]. During the process of making the sol, hydrolysis and condensation are two events that occur. Gel synthesis involves several chemical processes, including hydrolysis and condensation reactions of metal alkoxides lays the groundwork for variations in the rates of hydrolysis and condensation both occur. Throughout the process, results in various distinct polymer architectures, condensation, and hydrolysis go hand in hand. The pH and water ratio levels, temperature, type of catalyst, and concentration are the most critical elements that determine the speeds of the reactions [120].

2.5.2. Co-Precipitation

This technique calls for the addition of a basic solution (NaOH, NH_4OH, or urea) to a raw material in order to precipitate hydroxides, which is then followed by calcination in order to crystallize the hydroxide the painstaking management of particle size and particle distribution is one of the drawbacks the combination of particle size and uncontrolled precipitation frequently results in the production of macroparticles rather than nanoparticles [111].

2.5.3. Sonochemical Treatment

Sonochemical irradiation is an effective method for the synthesis of nanophase materials, as well as for the deposition and insertion of nanoparticles to and on supports consisting of mesoporous and ceramic materials, as well as polymers, this has been demonstrated through a series of experiments [112].

2.5.4. Micelle Method/Reverse Microemulsion

The reverse micelle method is a technique that has shown substantial control regarding the size distribution of nanoparticles in oxide environments this control has been established through a number of different experiments, at reverse micelles are water-in-oil emulsions in which the ratio of water to surfactant controls the size of the water clusters within which syntheses aqueous chemistry takes place and as a result controls the particle size that is produced as a result of the chemistry in other words the size of the water clusters determines the size of the particles that are produced. This method is especially useful for processes in an environment characterized by high temperatures, such as the precipitation of oxide [123].

2.5.5. Chemical Vapor Deposition

The chemical vapour deposition (CVD) process is a versatile method extensively used to coat huge amounts of surface in a relatively short time. This method is utilized regularly in the manufacturing of semiconductor ceramics and films, and it is done in a manner considered continuous. The CVD family is quite large and can be subdivided into subfamilies based on the differences in the activation technique, the pressure, and the precursors in the gas phase. The compounds, which can range from metals to oxide composites, are produced from a chemical reaction or the decomposition of a precursor [121].

PART 3

METHODOLOGIES

3.1. MATERIALS AND CHEMICALS

White cotton ($C_6H_{10}O_5$) n, Karabuk -Turkey), Gallium nitrate hydrate 98+ (Ga(NO3)3, Merck-Germany), Cobalt nitrate (Co(NO3)2, Merck-Germany), lanthanum nitrate hexahydrate (La(NO3)3, Merck-Germany), sodium hexahydrate (NaOH, soLab-Germany), L(+) ascorbic acid (C6H8O6, CarloEbra-France), ethanol absolute (C_2H_6O, IsoLab-Germany), distilled water. DMSO, LB medium and bacteriological agar were purchased from Sigma (Missouri, USA). For in vitro cell culture studies, a mouse fibroblast cell line (L929) was used. DMEM media was purchased from Biowest (Nuaillé, France). Deep Blue Company.

3.2. SAMPLES PREPARATIONS

The sample weighing 1 gr of cotton fabric was submerged in an aqueous sodium hydroxide solution for 5 minutes. After that, the material was removed from the solution and given many washes in distilled water until the ph became 7. The treated fabric was agitated for thirty minutes while submerged in an aqueous solution containing each of the three primary chemicals active (La^+, Ga^+, and Co^+) simultaneously with different concentrations each time (as in the order of the table below). After that, it was extracted from the solution and washed in distilled water until completely clean. The sample was submerged in an aqueous ascorbic acid solution and agitated for thirty minutes to imbue it with the primary actives. After the reaction was complete, the cotton was removed from the becker and washed with distilled water and ethanol. After that, it was dried in an oven at 65ºC. for an hour and a half.

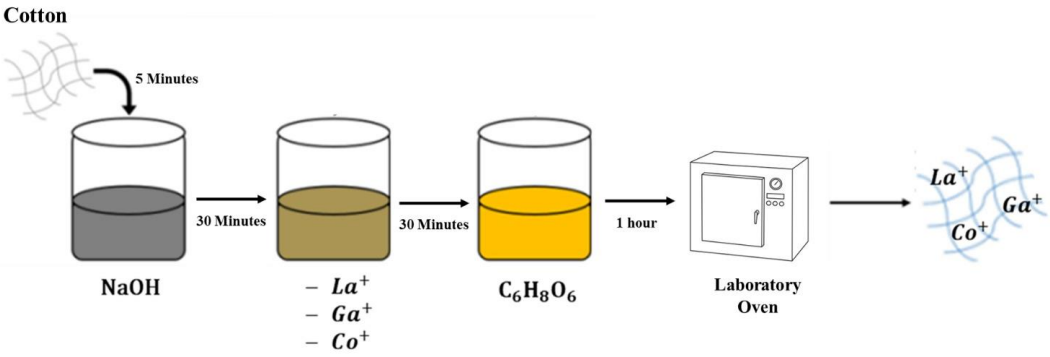

Figure 3.1. Process of coating the samples.

Figure 3.2. Prepared samples.

Table 3.1. Chemical concentration of the samples

Chemicals			**Concentrations**		
NaOH				6M	
$C_6H_8O_6$				0.01M	
1La t-Cot	**2La t-Cot**	**3La t-Cot**	0.01M	0.02M	0.04M
1Ga t-Cot	**2Ga t-Cot**	**3Ga t-Cot**	0.01M	0.02M	0.04M
1Co t-Cot	**2Co t-Cot**	**3Co t-Cot**	0.01M	0.02M	0.04M

3.3. CHARACTERIZATIONS

3.3.1. Crystal X R Diffraction

X-ray diffraction was utilized to look into the phase purity of the manufactured materials (XRD, Rigaku Ultima IV). To determine the lattice parameters, the samples were scanned from 20 to 80 degrees in 2 degrees, and an integrated software package was used. It was possible to determine the phase purity of all the materials by comparing them to standard patterns developed by the Joint Committee on Powder Diffraction and Standards (JCPDS).

3.3.2. Fourier-Transform Infrared Spectroscopy

Fourier-Transform Infrared Spectroscopy (FTIR, Bruker IFS 66/S) was utilized to provide conclusive evidence of the presence of functional groups. Transmission mode was used to record each spectrum, and the scanning range was set between -0 cm^{-1}.

3.3.3. Thermogravimetric Analysis

The thermogravimetric analysis, or TGA, was performed using a Perkin Elmer Pyris 1 apparatus at an ambient temperature of 950 ºC. To investigate the effects of temperature on the manufactured materials' thermal stability, variations in the sample weights were tracked as the temperature varied.

3.3.4. Scanning Electron Microscopy

Field emission scanning electron microscopy was utilized to examine particle size and shape (FESEM, Carl Zeiss Ultra Plus Gemini). A thin gold layer was applied to the samples beforehand to lessen the likelihood of sparking. Randomly selected particles were measured in size from FESEM images using the image analysis software ImageJ (National Institutes of Health, USA) to estimate the average particle size and particle size distribution.

Figure 3.3. Pluck gold Q150t Sample Preparation System.

3.3.5. Antimicrobial Activity Tests

Coated cotton extracts were tested for antimicrobial efficacy against Staphylococcus aureus. The 0.04 M ion doped groups (30 mg) were inserted in 15 ml falcon tubes. Each sample was immersed in 70% ethanol for 2 hours, then exposed to UV radiation for 30 minutes to sterilize. After the samples were dry, 2 ml of LB broth was added and incubated at 37°C for 24 hours. After 24 hours, 100 l of sample extracts were transferred to a 96-well plate. The turbidity of sample groups was measured at 410 nm wavelength to determine bacteria growth using a VarioSkan® Flash (Thermo Fischer) multimode reader. Control groups were fresh LB Broth and inoculated LB Broth. LB agar was tested for disk diffusion. 30 mg of each sample was pushed into a 96-well plate bottom (radius 4.5 mm). Each disk sample was placed on LB agar Petri dishes with Staphylococcus aureus bacteria. Antimicrobial activity was tested by incubating Petri dishes at 37°C overnight.

3.3.6. Cytotoxity Test

A mouse fibroblast cell line was used for in vitro investigations (L929). Cells were grown in DMEM high glucose media with 10% FBS and 1% penicillin-streptomycin in a CO_2 incubator (5% CO_2, 95% humidity, 37 °C). 2 mg of cotton was put on 96-well plates to test cell viability. Samples were sterilized in 70% ethanol for 2 hours and UV light for 30 minutes. Overnight in the growing medium. Five thousand cells/well were seeded on the scaffold surface in 20 l of medium and incubated at 37

°C for 2 h for initial adhesion. After culture, 100 l of DMEM was added to wells and cell viability was measured with Deep Blue Assay. At intervals, 10 l of Deep Blue Assay solution was added to wells and incubated for 3 hours. After incubation, 100 l of fluid was transferred to a fresh plate, and optical densities were measured at 530 and 590 nm (Reference for Deep Blue). SEM analyzed cell attachment and morphology in groups. In 96-well plates, sterile sample groups were seeded with 10,000 L929 cells/well. After 7 days, samples were rinsed with PBS and fixed with 4% paraformaldehyde in PBS for 15 minutes. After two PBS rinses, groups were exposed to EtOH (30, 50, 70, 80, 90, and 100%) for 10 min. Parafilm-wrapped samples at 4 °C.

.

PART 4

RESULT DISCUSSION

4.1. CHARACTERIZATIONS OF LANTHANUM–COATED COTTON COMPOSITES

4.1.1. XRD

In Figure 4.1 example of the natural cellulose I polymorph can be seen in the untreated sample's diffractogram, which has two prominent peaks located at 2Θ =15.5° and 2Θ =23.3°. These peaks correlate to the crystallographic planes of cellulose I and are: (110), (020) typical of natural cellulose I polymorph similar result was reported by [114,116]. Pure NaOH and $C_6H_8O_6$ treated samples exhibit peaks at 2Θ =12.4° and 2Θ = 23.3° diffractogram peaks for the regenerated cellulose samples are quite close to those for polymorphic cellulose II with plane (101) and (002) [117] It has been discovered that both pure NaOH and water facilitate the transformation of cellulose I into cellulose II during the regeneration process [118]. However, after adding (La $(NO_3)_3$ peaks are not distinctive. It could be due to the fact that low-intensity reflections are a probable reason for the indistinguishable background noise in the XRD. The weight is low, and the Bragg peaks for the minor phase will be very faint and may not appear in the XRD pattern at all.

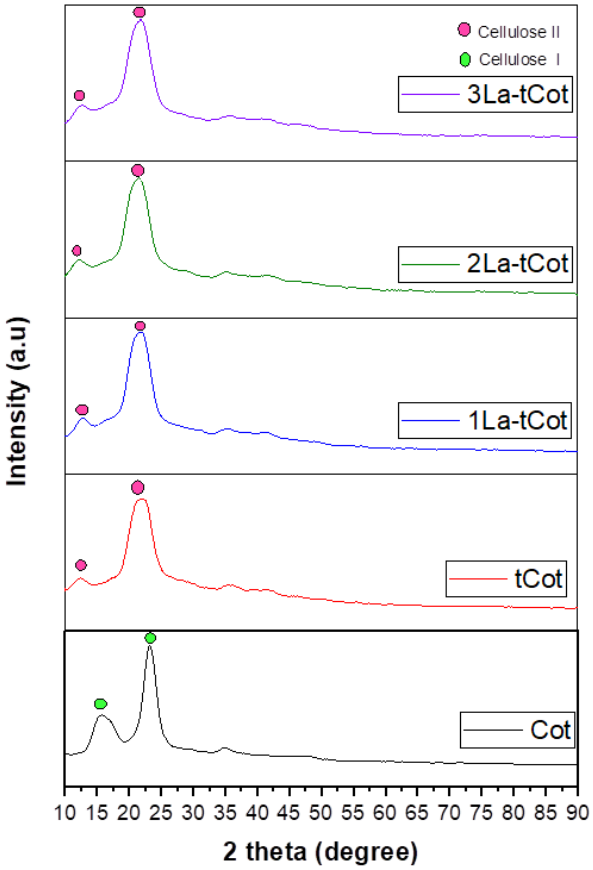

Figure 4.1. Presents an illustration of the XRD pattern of cottons that have been coated with $La(NO_3)_3$.

4.1.2. FTIR

In figure 4.2 the C–H stretching is the reason for of the bands at 2824 cm^{-1} in frequency[119]. Absorption band 1313 cm^{-1} is attributed to cellulose II's CH bending vibration. [120]. Diagnostic spectral peaks could be seen in the spectra of the natural cellulose at a frequency of approximately 1150 cm^{-1}. These peaks were caused by C-O stretching vibrations [121]. The C-O-C glycosidic ether band may be seen at a frequency of 1105 cm^{-1} and is caused by the polysaccharide components, the majority of which are cellulose [122]. (S–S) stretching vibrations were determined to be the cause of the peak at 658 cm^{-1} [123], essential for the production of amino acids by cotton plants [124]. The stretching vibrations of OH groups are due for the peak that can be found at 3744 cm^{-1} [125]. The band that may be found close to 897 cm^{-1} is associated with the CH distortion of -glycosidic links, that is in turn connected to the quantity of amorphous cellulose [126]. OH, has a force constant of 599 cm^{-1} for

intermolecular hydrogen bonding accordingly [127]. The range around 430 cm^{-1} might be interpreted as a sign of the coordination between the metal ions and oxygen correspondingly [128]. The FTIR spectra show some proof that the alkali treatment of the fibers caused the conversion of celullose I to cellulose II.

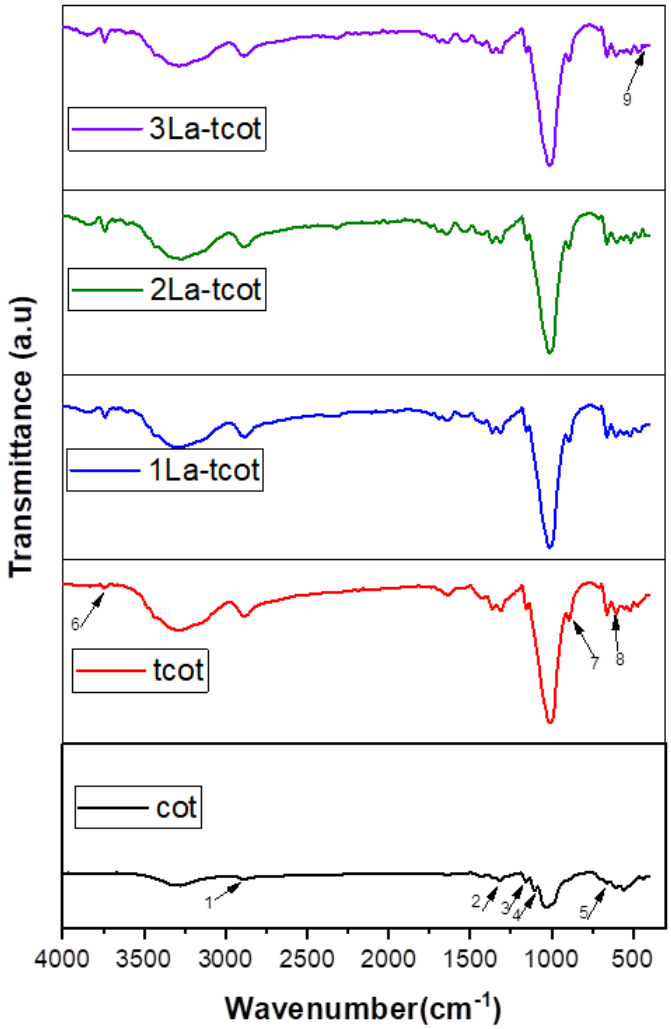

Figure 4.2. FTIR characteristic peaks of samples treated with $La(NO_3)_3$.

Table 4.1. Characteristics peak of FTIR samples treated with $La(NO_3)_3$

Peak number	Wavelength (cm^{-1})	Band assignment
1	2884	CH
2	1313	CH
3	1150	C-O
4	1105	C-O-C
5	658	S–S
6	3744	OH
7	897	CH
8	600	OH
9	430	M–O

4.1.3. Field Emission Scanning and Energy Dispersive X-Ray Analysis

The SEM images of the pure cotton show no visible particles, only closely packed microfibrils but SEM photographs of fabric treated with NaOH $C_6H_8O_6$ and La $(NO_3)_3$, exhibit agglomerate, as illustrated in Figure 4.3 because of the formation of these crystallized nanoparticles on the surface of the cotton from the weakly crystalline solids the fibres of the cotton end up having an uneven shape. The qualitative EDX analysis allows for the identification of peaks that correspond to the elements that are present in a sample when those peaks occur in a spectrum that was produced as a result of the inspection that the sample was exposed to the signal strength is proportional to the concentration of that element in the sample. Still, the energy center at which a peak emerges is specific to each component. The presence of hydrogen (H), carbon (C), oxygen (O), and sodium (Na) was found chemically in the sample that was treated only with NaOH and $C_6H_8O_6$ and the presence of Lanthanum nitrate $La(NO_3)_3$ grew proportionally when the concentration was raised (figure 4.3).

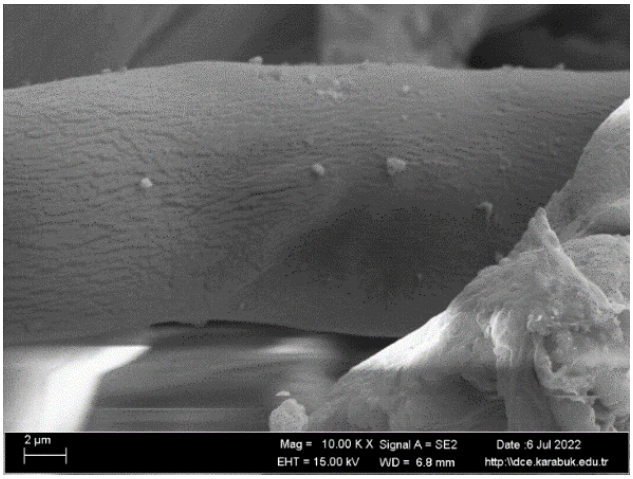

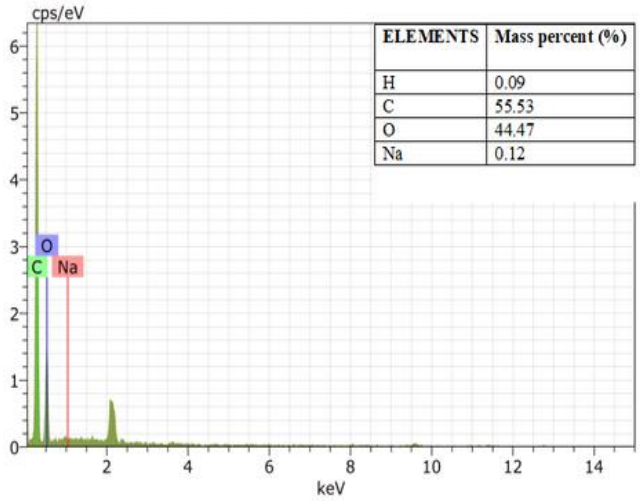

a)

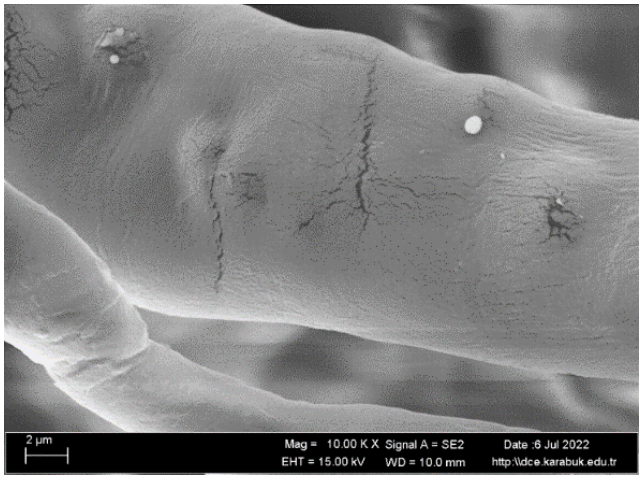

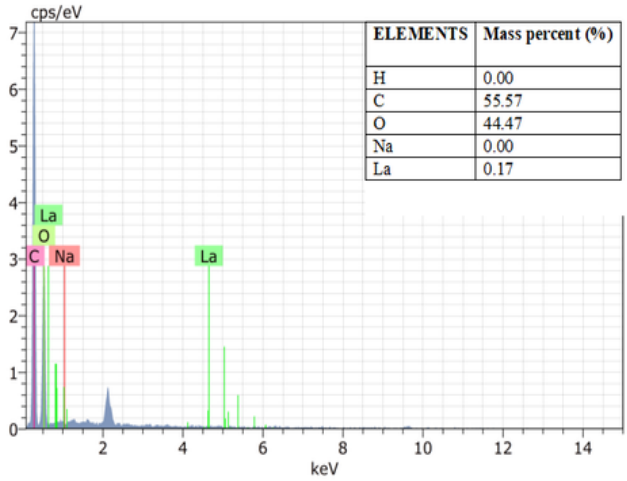

ELEMENTS	Mass percent (%)
H	0.00
C	55.57
O	44.47
Na	0.00
La	0.17

b)

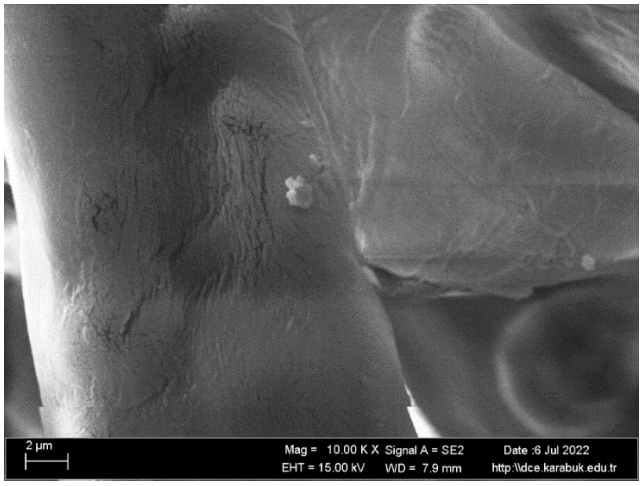

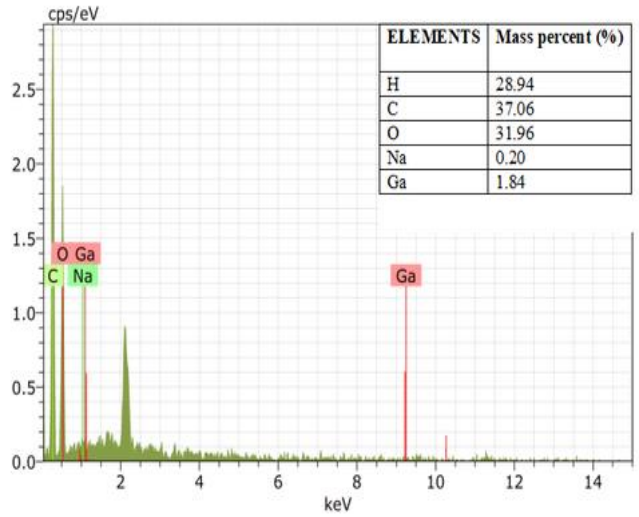

ELEMENTS	Mass percent (%)
H	28.94
C	37.06
O	31.96
Na	0.20
Ga	1.84

c)

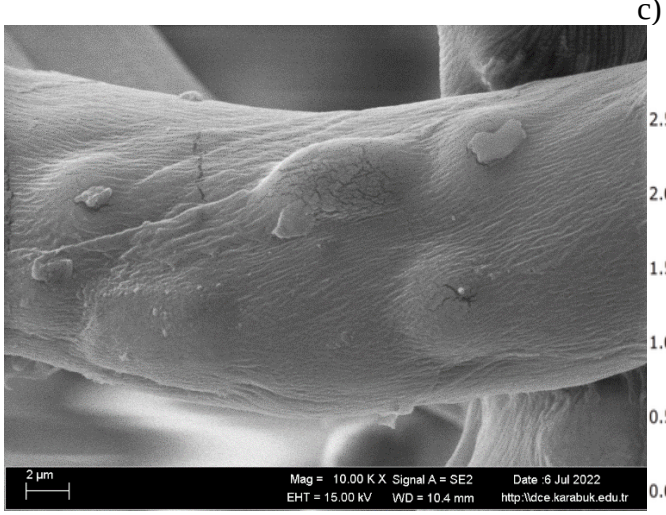

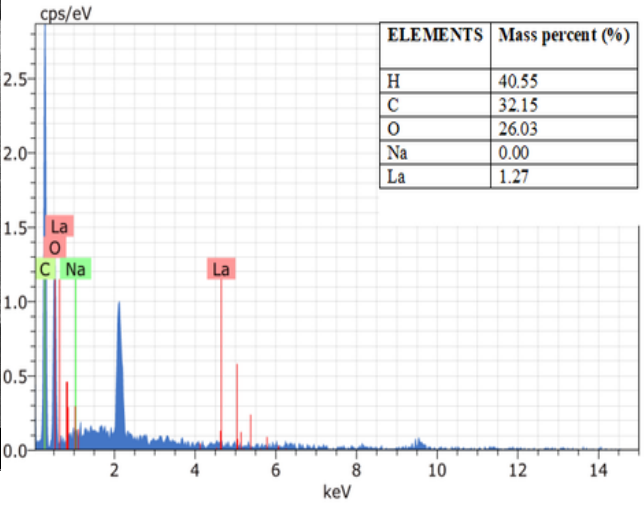

ELEMENTS	Mass percent (%)
H	40.55
C	32.15
O	26.03
Na	0.00
La	1.27

d)

Figure 4.3. a) sem and edx of NaOH treated sample, b) sem and edx of 1La-tcot treated sample, c) sem and edx of 2La-tcot treated sample, d) sem and edx of 3La-tcot treated sample.

4.1.4. Thermogravimetric Analysis

Figure 4.4. displays the results of an analysis conducted on the thermal characteristics of the untreated sample to lose almost 5% of its weight between 32°- 140° C, the second stage of breakdown, which result in approximately a loss of 82% of the weight at temperatures in the range of 200°- 380° C was caused by the decomposition alpha-cellulose primary component of cotton fibres [129]. The sample that was treated with NaOH $C_6H_8O_6$ between 30°- 91° C experienced a weight loss of approximately 7%, and during the second stage, 75% of this weight dissolved between 94°- 360° C (Effect of Mercerization on the Properties of Pandanus Odorifer Lignocellulosic Fibre). The sample that was treated with NaOH $C_6H_8O_6$ and merely 0.01M of La $(NO_3)_3$ between 30°- 130° C saw a loss of approximately 7% of its weight, and during the second stage, 75% of this weight dissolved between 138°-360° C. The sample that was treated with NaOH $C_6H_8O_6$ and just 0.02M of La $(NO_3)_3$ at temperatures ranging from 30°- 130 ° C saw a loss of roughly 10% of its weight, and 78% of this weight was dissolved during the second stage, which took place at temperatures ranging from 120°- 360° C. The sample that was treated with NaOH $C_6H_8O_6$ and merely 0.04M of La $(NO_3)_3$ lost approximately 6% of its weight between the temperatures of 28°-130°C and between the temperatures of 130°- 360°C, 81% of the weight had disappeared. TGA curves show the weight loss of the sample that was treated with La $(NO_3)_3$ is almost the same as the weight loss of the NaOH and $C_6H_8O_6$ sample. Still, it is less than the weight loss of the untreated cotton, which could be attributed to the free water volatilization attaching water to the cotton [130].

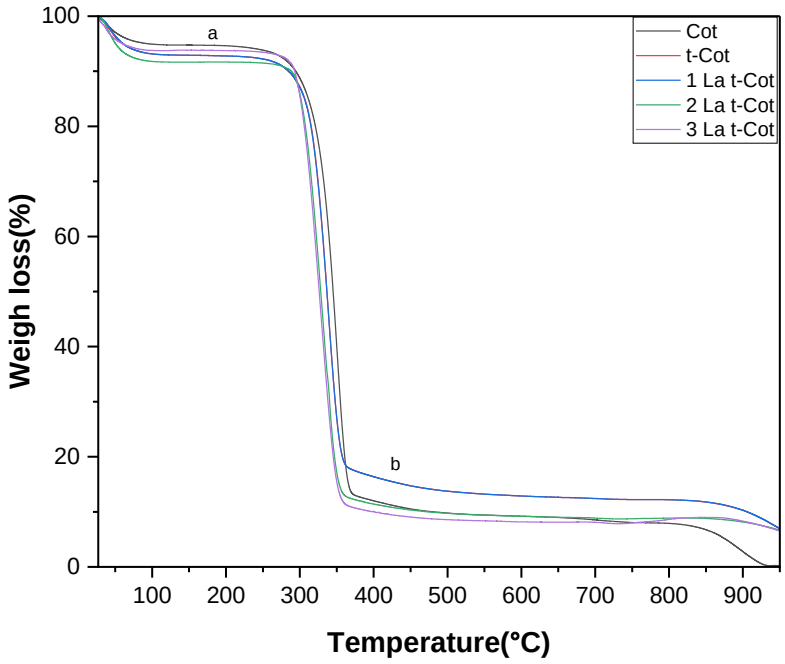

Figure 4.4. Thermograms of samples treated with $La(NO_3)_3$

4.2. CHARACTERIZATIONS OF COBALT

4.2.1. XRD

In figure 4.5 the natural cellulose I polymorph can be seen in the untreated sample's diffractogram, which has two prominent peaks positioned at 2Θ =15.5° and 2Θ = 23.25° This is a typical example of the natural cellulose I polymorph consistent with the crystallographic planes of cellulose I (110), (020) [114,116]. Peaks at 2Θ =12.4° and 2Θ =21.4° can be seen in the material that was only treated with NaOH and $C_6H_8O_6$. These peaks can be detected around the diffraction angles of (110), (020)° [131], the regenerated cellulose samples have diffractogram peaks that are comparable to those seen for polymorphic cellulose II, it has been observed that both pure NaOH and NaOH-urea systems enable a transition from cellulose I to cellulose II [118]. After the addition of Co $(NO_3)_2$ there is no clear peak and the undetectable background noise in the XRD may have been caused by low-intensity reflections.

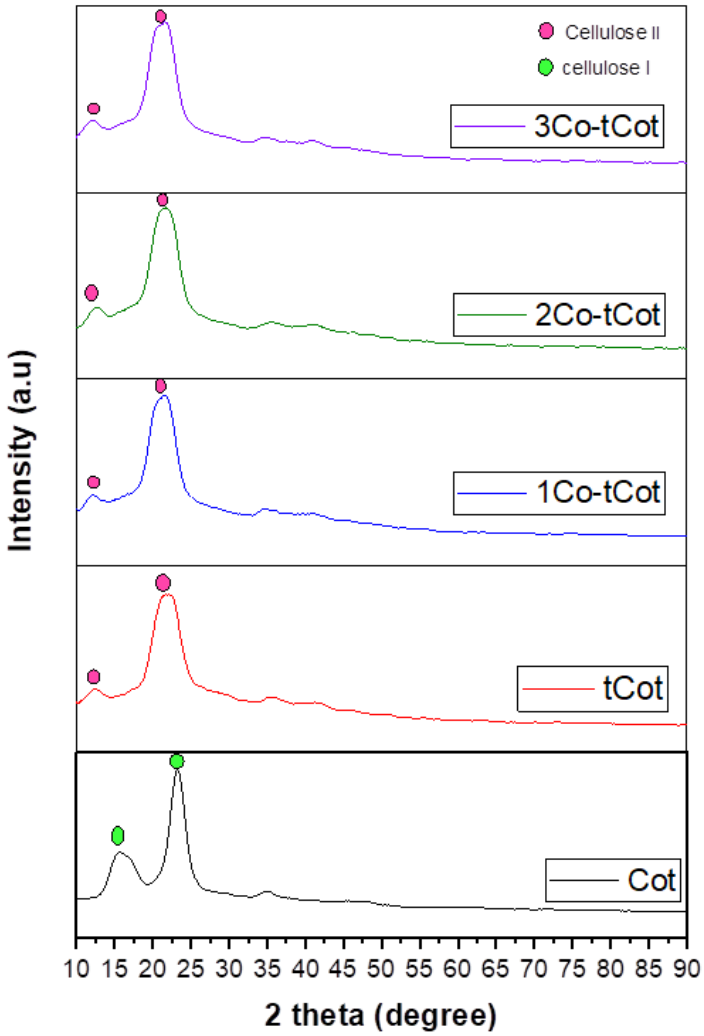

Figure 4.5. Presents an illustration of the XRD pattern of cottons that have been coated with $Co(NO_3)_2$

4.2.2. FTIR

In figure 4.6, the band at 1437 cm^{-1}, which is caused by the C–H bending on methyl and methylene [132]. 1323 cm^{-1} is attributed to the Primary or secondar (O–H) [133]. thus says [134] the C-N stretching vibrations is linked to the 1166 cm^{-1} band. The C-O-C group is responsible for the spectral line at 1107 cm^{-1} [135].

The bands at 662 cm^{-1} are caused by the O-H bending occurring outside of the plane [136]). The C=N stretching was found to be responsible for the peaks in the FTIR spectra that appeared at 601 cm^{-1} [137] naturally present in natural cellulose sources [138]. The symmetric aliphatic C-H bending vibration is responsible for the peak at a

frequency of 1370 cm^{-1} [139]. C-O-C deformation vibration absorption peaks about 1158 cm^{-1} were detected in both xylem and bark, confirming the presence of cellulose and hemicellulose in these tissues [140, 141]. The bands that were detected at a frequency of 885 cm^{-1} are associated with C-H out of plane bending vibrations [133], [142]. The value of 518 cm^{-1} could be attributed to C-H bending that occurs outside of the plane [143]. the hydroxyl group in cellulose is responsible for the prominence at 3748 cm^{-1} [144]. The peak at of 428 cm^{-1} that was found might be attributed to the presence of metal oxide stretching vibration [145]

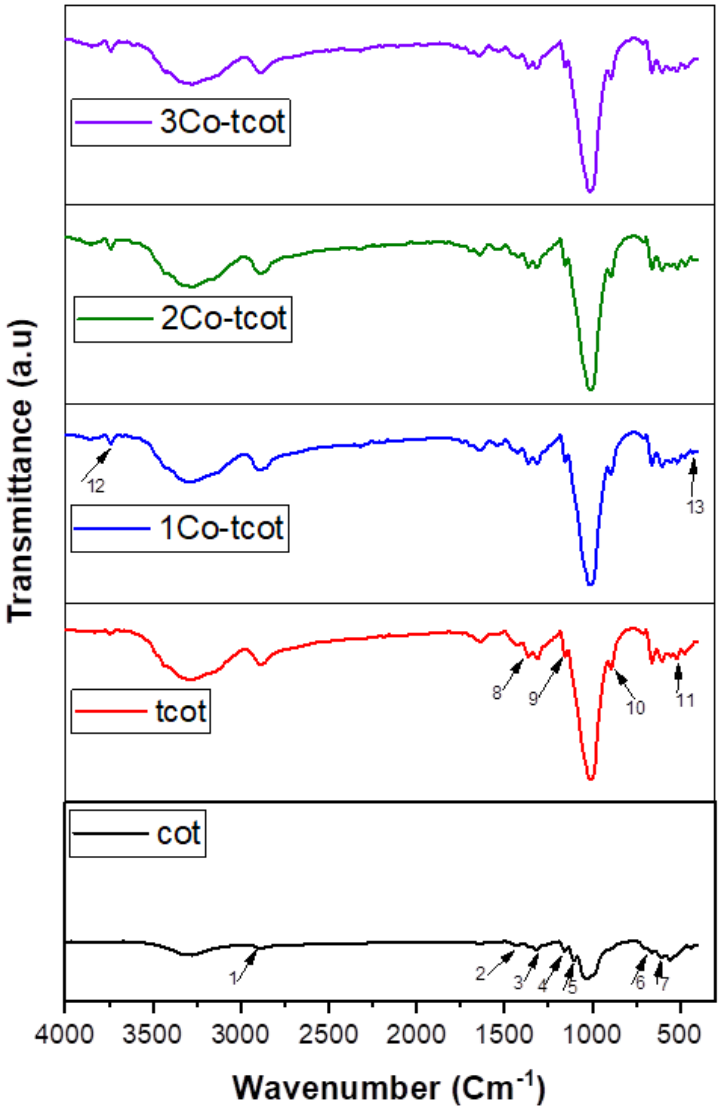

Figure 4.6. FTIR characteristic peaks of samples treated with $Co(NO_3)_2$

Table 4.2. Characteristics peak of FTIR samples treated with $Co(NO_3)_2$

Peak number	Wavelength (cm^{-1})	Bande assignment
1	2908	C-H
2	1437.9	C–H bending
3	1323.7	O–H
4	1166.6	C-N
5	1107.5	C–O–C
6	662.87	O–H
7	601.6	C=N
8	1370.6	C-H
9	1158.5	C-O-C
10	885	C-H
11	518	C-H
12	3748	OH
13	428	M–O

4.2.3. Field Emission Scanning and Energy Dispersive X-Ray Analysis

SEM photos of pure cotton fabric reveal no visible particles, whereas those of fabrics treated with NaOH, $C_6H_8O_6$, and Co $(NO_3)_2$ display agglomerate, the scanning electron micrographs of the samples shown in the Figure 4.7 exhibit the formation of crystallized nanoparticles on the surface of the cotton from the weakly crystallized solids these fibers have an irregular shape. Peaks corresponding to the elements present in a sample are identified through qualitative EDX analysis when they appear in a spectrum generated by the inspection to which the sample was subjected. The energy center at which a peak appears is unique to each element, while the signal strength is proportional to the concentration of that element in the sample. Four elements (hydrogen (H), carbon (C), oxygen (O), and sodium (Na)) were discovered chemically in the sample treated just with NaOH and $C_6H_8O_6$ (figure 4.7.)

And the presence of Co $(NO_3)_2$ increased proportionally with increasing concentration (figure 4.7).

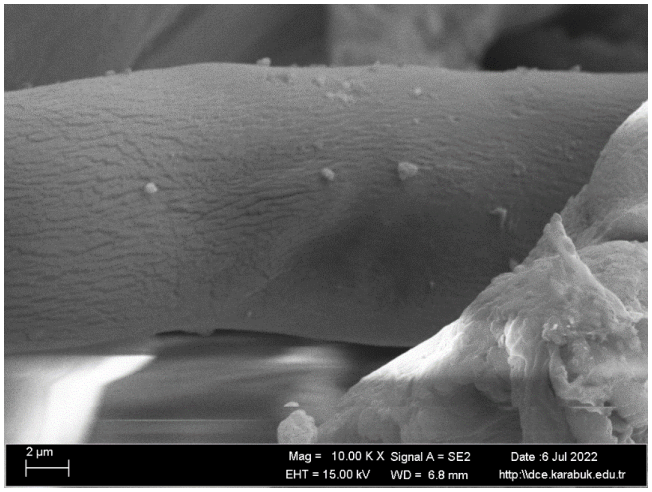

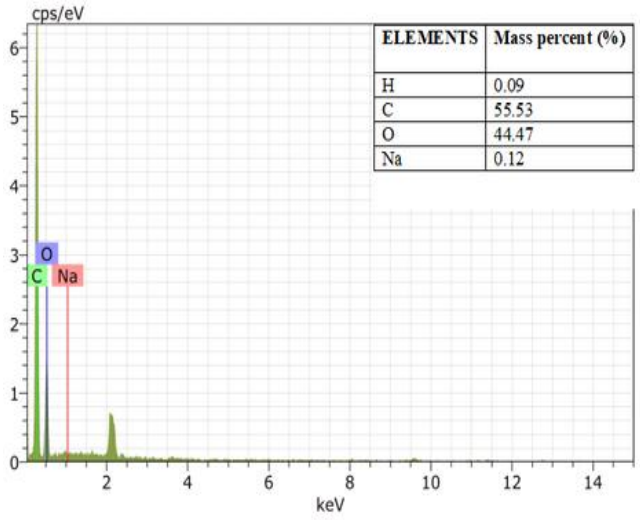

ELEMENTS	Mass percent (%)
H	0.09
C	55.53
O	44.47
Na	0.12

a)

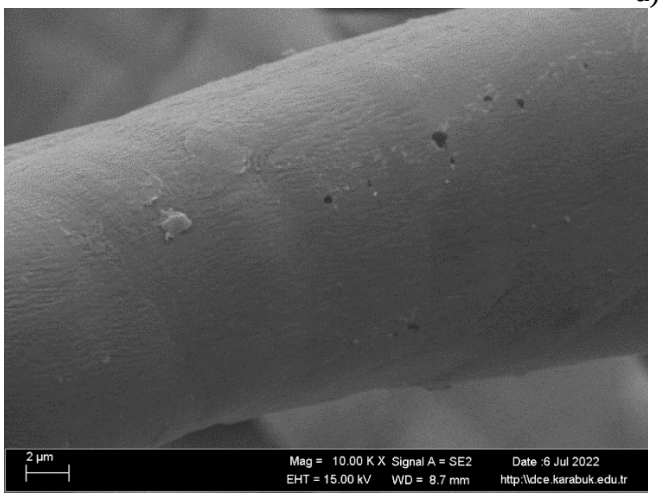

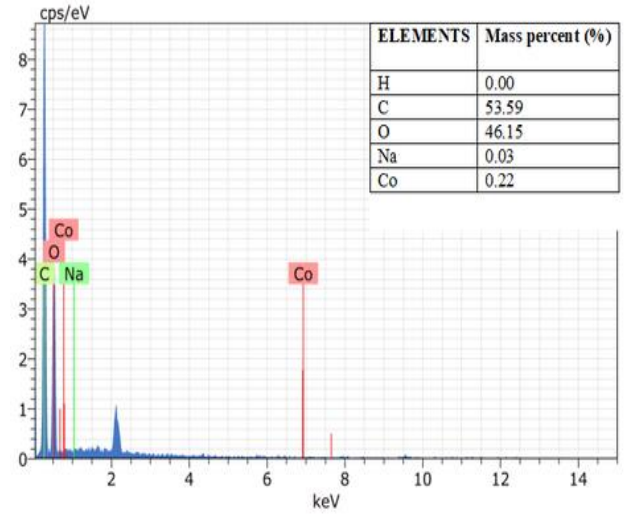

ELEMENTS	Mass percent (%)
H	0.00
C	53.59
O	46.15
Na	0.03
Co	0.22

b)

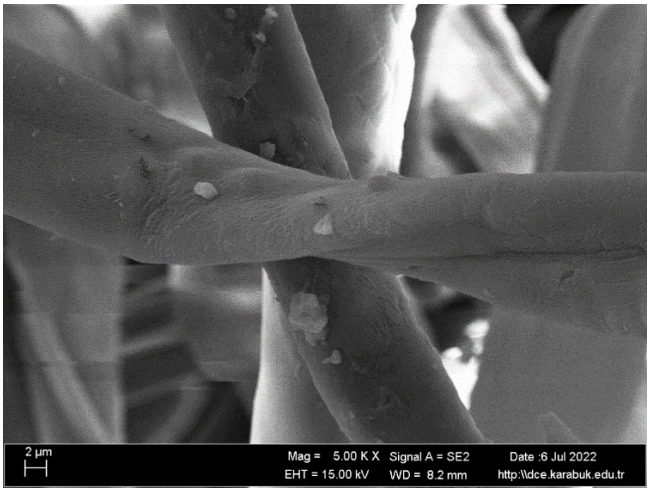

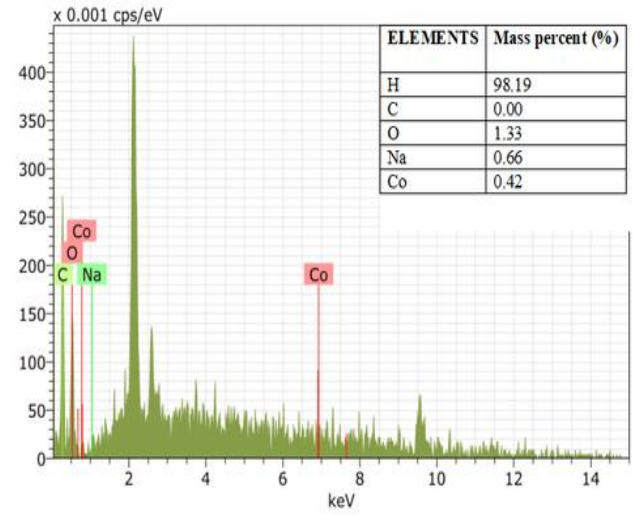

ELEMENTS	Mass percent (%)
H	98.19
C	0.00
O	1.33
Na	0.66
Co	0.42

c)

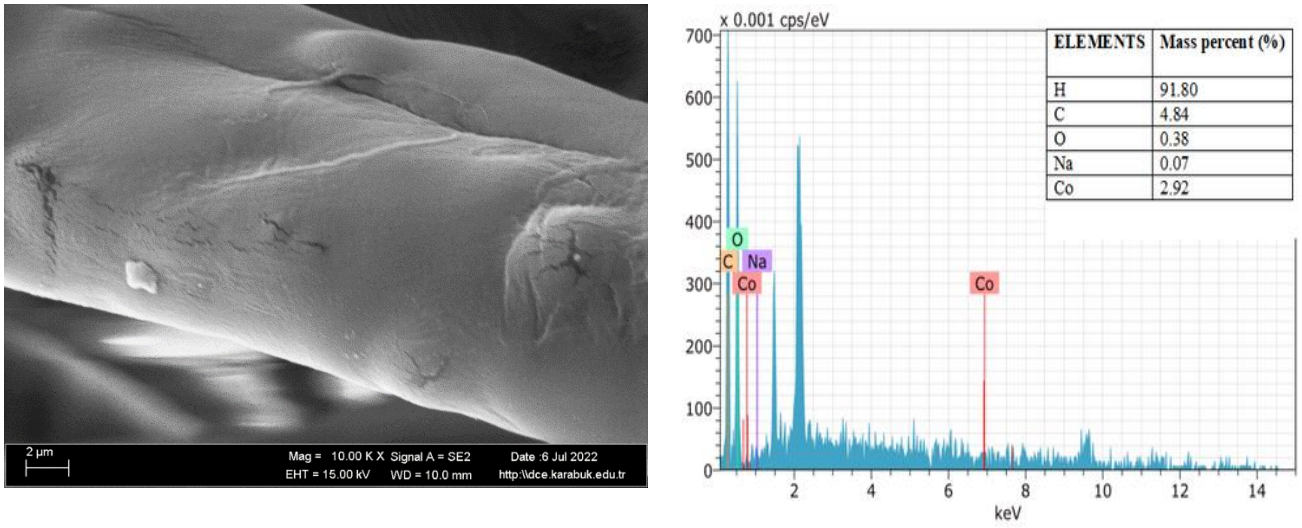

d)

Figure 4.7. a) sem and edx of NaOH treated sample, b) sem and edx of 1Co-tcot treated sample, c) sem and edx of 2Co-tcot treated sample, and d)sem and edx of 3Co-tcot treated sample.

4.2.4. Thermogravimetric Analysis

Figure 4.8 displays the outcomes of a thermal analysis performed on the samples., the untreated sample lost almost 6% of its weight between 32°-150 °C between 200°-370°C the second phase of degradation in which 82% was lost. Between 30°- 91° C, the sample treated with NaOH $C_6H_8O_6$ lost about 7% of its weight; between 94°-360° C 75% of this weight was dissolved. The experimental sample underwent treatment with NaOH $C_6H_8O_6$ and Co $(NO_3)_2$ at a concentration of 0.01M, within a temperature range of 27°- 94 ° C the results indicated a weight loss of approximately 7% during the subsequent stage which occurred between 100°- 370° C 77% of the initial weight was observed to dissolve. The experimental sample that was treated with NaOH $C_6H_8O_6$ and Co $(NO_3)_2$ at a concentration of 0.02M within a temperature range of 30°-100 °C showed a weight loss of approximately 6%, and during the subsequent stage, which took place at temperatures ranging from 120°-370°C, it was observed that 79% of the sample's initial weight dissolved. At temperatures ranging from 30°-86° C, the experimental sample treated with NaOH $C_6H_8O_6$ and a concentration of 0.04 M Co $(NO_3)_2$ showed a weight loss of approximately 6%, during the second stage 79% of the total weight dissolved between temperatures of 140°-370°C. The thermal

decomposition includes different stages: the first stage involved the release of adsorbed water, which started at around 100 degrees Celsius; the second stage was a fast reduction during which decarboxylation and dehydration delivered flammable gasses such as ketones aldehydes and ether [146].

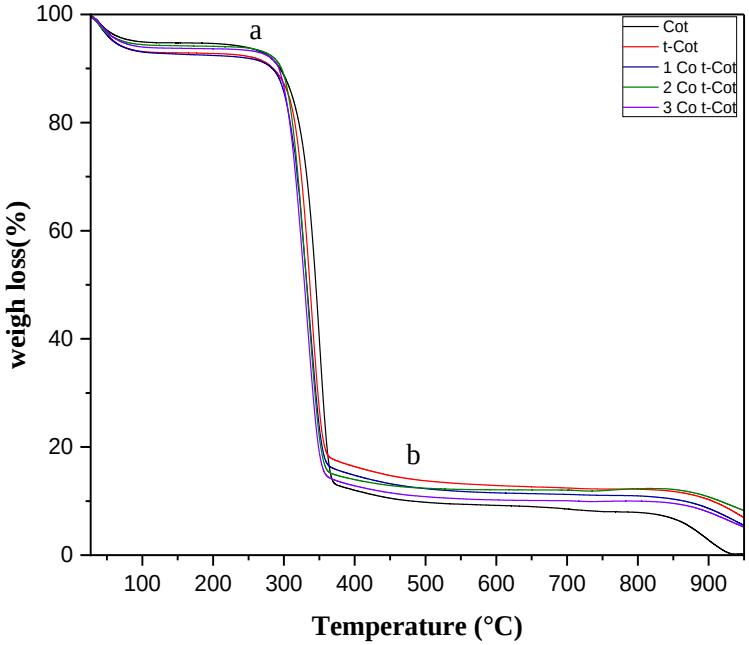

Figure 4.8. Thermograms of samples treated with $Co(NO_3)_2$

4.3. CHARACTERIZATION OF GALLIUM

4.3.1. XRD

In Figure 4.9, two different values can be seen in the X-ray diffraction peaks of pure cotton 2Θ =15.5° and 2Θ=23°. This X-ray pattern illustrates the usual presentation of diffraction peaks that are associated with the crystalline structure of cellulose [147], [148]. After treatment with NaOH and $C_6H_8O_6$, the analysis by diffractometry show the appearance of two new peaks 2Θ=12°, 2Θ =21° may have caused by the alkanization [149], also after adding $(Ga(NO_3)_3$ concentration, there is a small recognizable peak at 42 appears for the samples treated with 2Ga-tCot, 3Ga-tcot. This characteristic lines can be attributed to the presence of Ga nanoparticles [150,151].

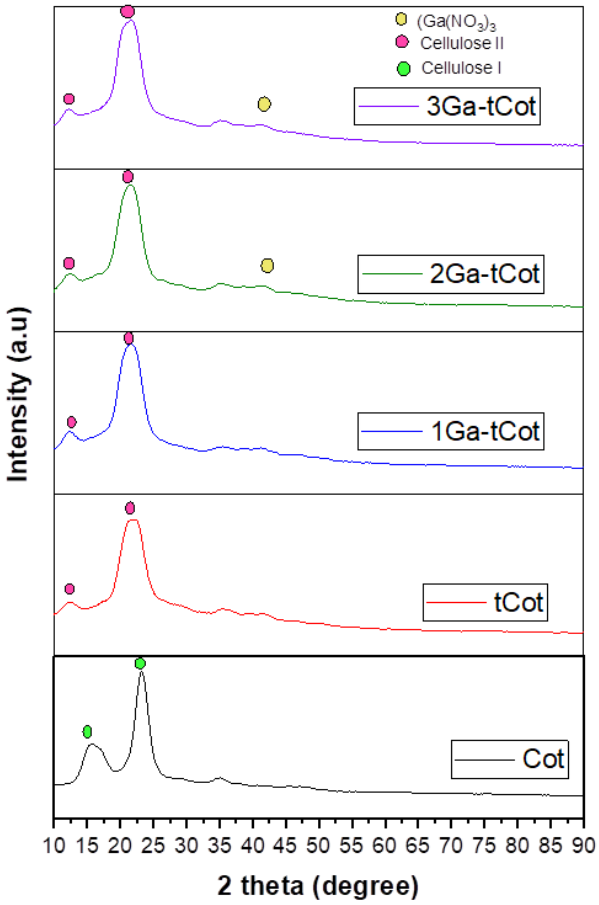

Figure 4.9. Illustration of the XRD pattern of cottons that have been coated with($Ga(NO_3)_3$

4.3.2. FTIR

In figure 4.10 O–H stretching waves cause the frequency at 3740 cm^{-1} [152]. At a wave number of 2879 cm^{-1}, there is a vibration from C-H that stretches [153] peak at 1370 cm^{-1} may be attributed to CH_2 twisting in cellulose and hemicellulose [154,155]. Peak at 1315 cm^{-1} is attributed to CH_2 [156]. The absorption spectra of lip mucosa were examined using Fourier transform infrared spectrometry, and the results showed that two wavelengths, 1152 cm^{-1} for glucose absorption [157]. Also, it is important to note that the utilization of citric acid as the crosslinker results in the development of an ester bond (C–O–C) between the OH groups that are present in the two polymers and the COOH groups that are present in the citric acid [158]. At a wave number of 2879 cm^{-1} there is a vibration from C-H indicating that absorption is taking place [159]. FTIR spectra still displayed the transmission peak at 1370–1470 cm^{-1} because uncrosslinked

=C–H persists at the ends of the branches [160]. The emissions of both CH_2 and CO can be seen as bands between 1500 and 1200 cm^{-1} [161]. A carbon-based developed at 885 cm^{-1} perhaps associated with the alkaline treatment and the ascorbic acid-based redox reduction. The spectra 603cm^{-1} is related to gypsum [162], research results could possibly be related Application of Gypsum to agricultural soils has been shown to increase plant development as it is a fairly soluble source of the critical plant nutrients, calcium, and sulfur [163]. It's possible that the peak at 518 cm^{-1} is due to the asymmetric stretching of C=O groups [164]. This last band 440.5 cm^{-1} is presence is triggered by the presence of metal oxide.

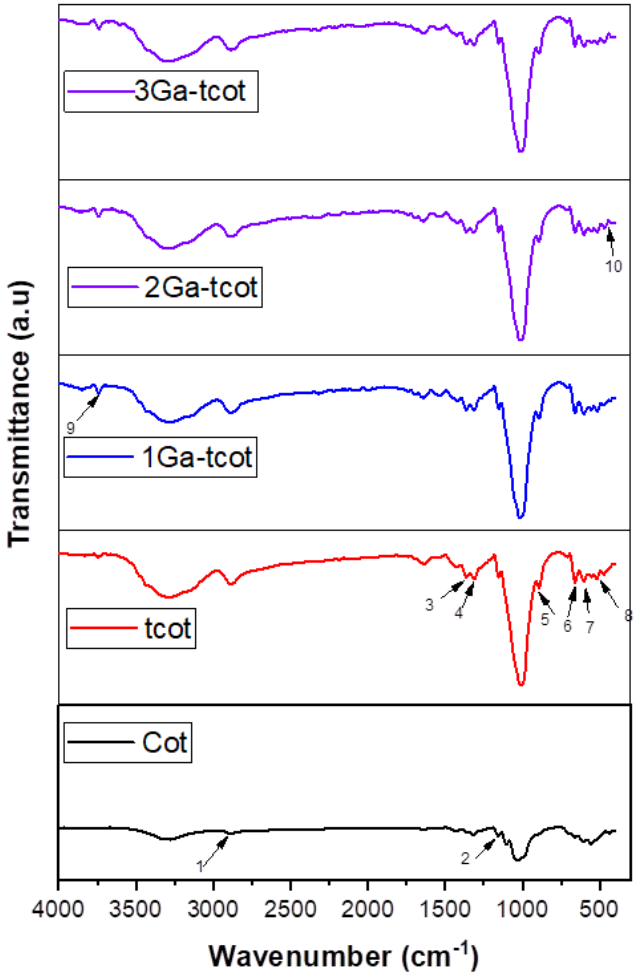

Figure 4.10. FTIR peaks of samples treated with $(Ga(NO_3)_3$

Table 4.3. Characteristics peak of FTIR samples treated with ($Ga(NO_3)_3$

Peak Numbers	Wavelength(cm-1)	Bande assignement
1	3740.68	O–H
2	2879	C–H
3	1370	CH_2
4	1315	CH_2
5	1152	C–O–C
6	885	C-O-O-
7	657	C-H
8	603	$CaS0_4$
9	518	C=O
10	440.5	M–O

4.3.3. Field Emission Scanning Electron Microscopy and Energy Dispersive X-Ray Analysis

The SEM images (figure 4.11) showed that the cotton fabrics were coated by globular nanaopetiles which could be due to deposition of gallium metal nanoparticles. External morphology is in the form of spheres ranging from nanometers to micrometers. The samples were analyzed with EDX to establish their make-up and composition, and the presence of the chemical element NaOH, $C_6H_8O_6$, Ga was observed in the EDX after using precipitation methods for coating on the samples. In the presence of the chemical element Ga $(NO_3)_3$, the NaOH solution can be utilized for the preparation of regenerated cellulose by the use of inorganic cellulose dissolving systems.

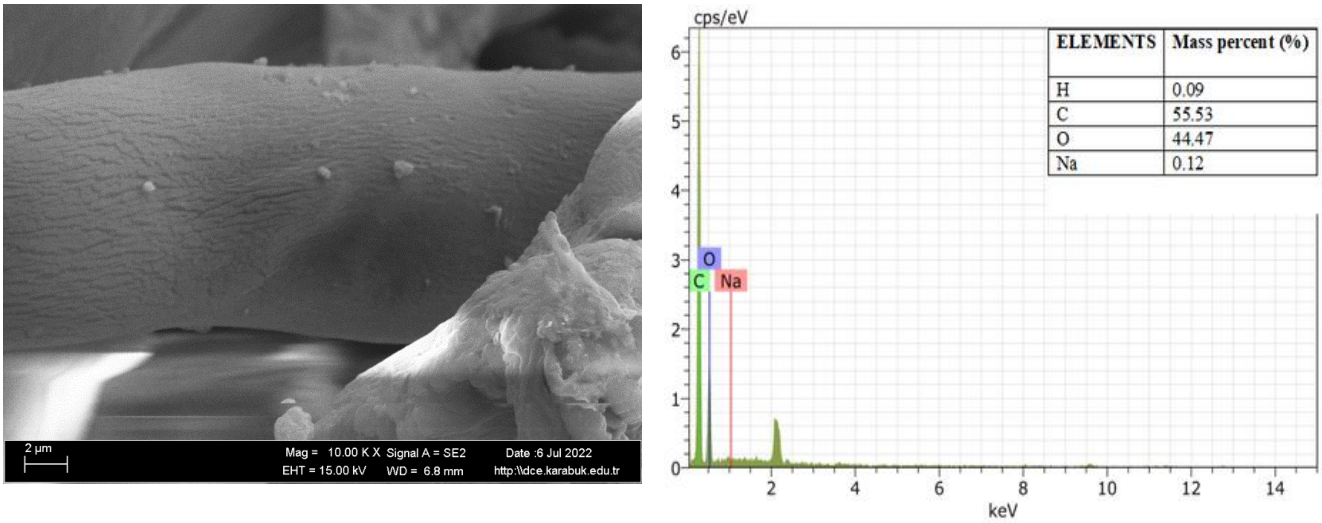

a)

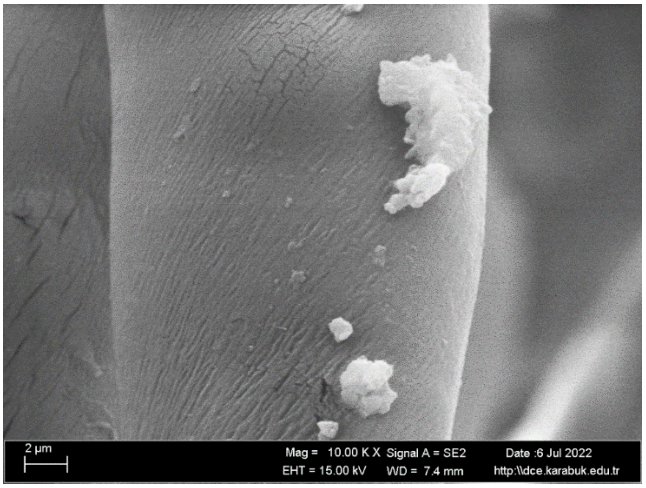

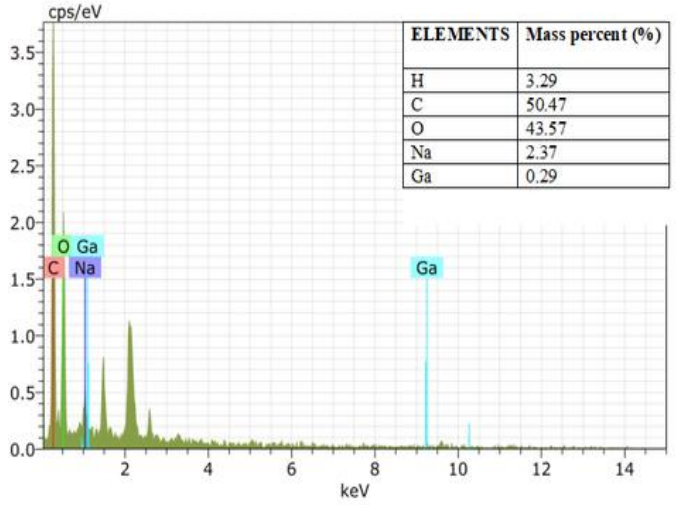

b)

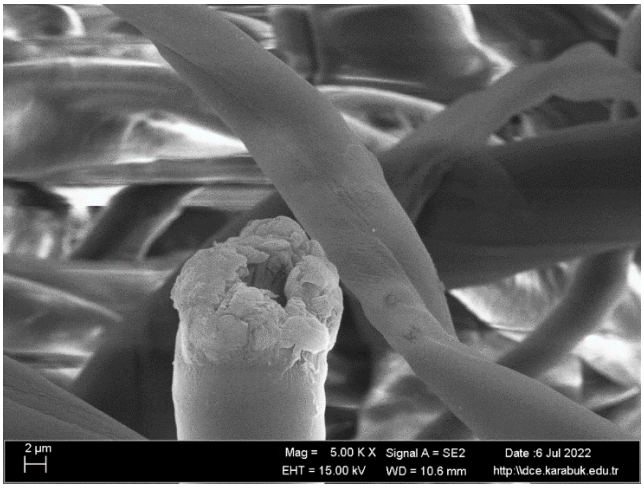

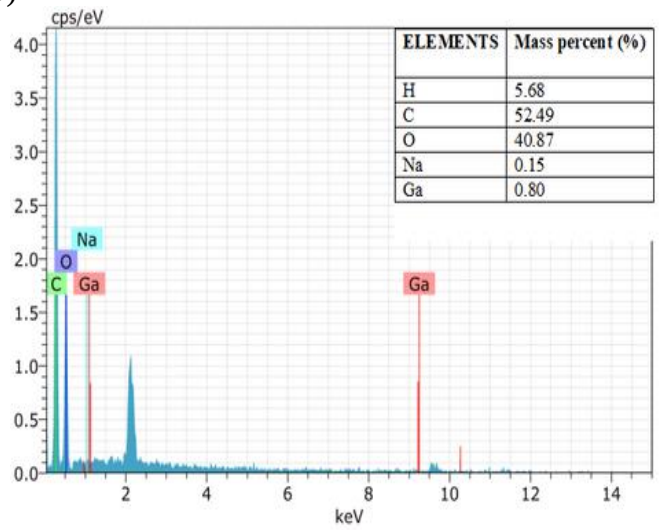

c)

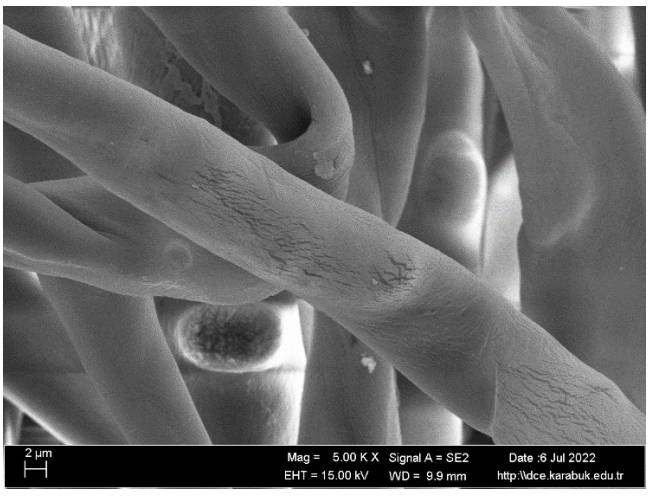

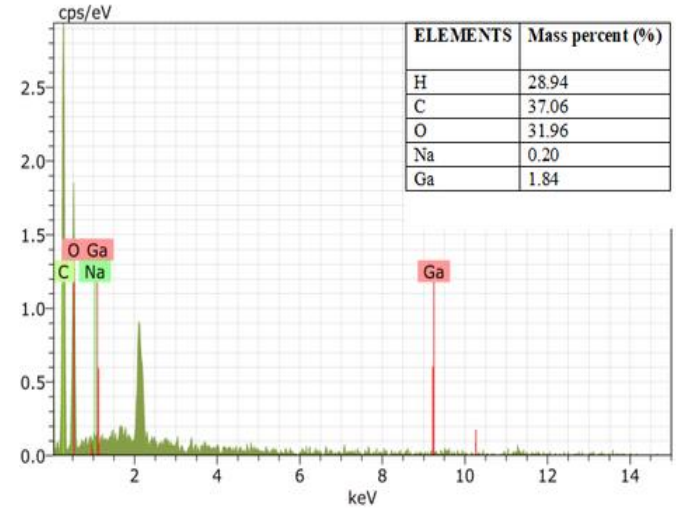

d)

Figure 4.11. a) sem and edx of NaOH treated sample,b) sem and edx of 1Ga-tcot treated sample,c) sem and edx of 2Ga-tcot treated sample, d)sem and edx of 3Ga-tcot treated sample.

4.3.4. Thermogravimetric Analysis

Results from a thermal analysis of the modified samples are presented in Figure 4.12. The untreated sample to lose nearly 6% of its weight between 32°-150° C, the second phase of the degradation process, which took place between temperatures of 200°-370°C. The sample that was handled with NaOH, $C_6H_8O_6$ experienced a loss of approximately 7% of its weight between the temperatures of 30°- 91° C, between the temperatures of 94°- 360° C approximately 75% of this weight was dissolved. A weight loss of approximately 6% was observed in the experimental sample that was treated with NaOH, $C_6H_8O_6$, and Ga $(NO_3)_3$ at a concentration of 0.01M within a temperature range of 30°-95°C. In the second phase, between 150°-370° C , it came out that 78% of the sample's original weight was dissolved. The experimental sample that was treated with NaOH, $C_6H_8O_6$, and Ga $(NO_3)_3$ at a concentration of 0.02M within a temperature range of 26°-110° C showed a weight loss of approximately 6% in the second phase which took place between 150°- 360° C, it was found that 78% of the sample's original weight was dissolved. A weight loss of approximately 7% was observed in the experimental sample that was treated with NaOH $C_6H_8O_6$ and $Ga(NO_3)_3$ at a concentration of 0.04M within a temperature range of 27°-11O° C. It was discovered that 79% of the sample's initial weight disappeared during the second phase, which took place at temperatures ranging from 150°- 360°C. Visible variations can be observed in the way modified cellulose experiences thermal degradation, when temperatures reach approximately 150°C, the predominant mass loss is always attributed to the release of volatile materials [166,167]. The second step in the decomposition process is the thermal degradation of cellulose, and it can take place at a variety of temperatures, with the starting point originating anywhere from 200° to 400°C[168].

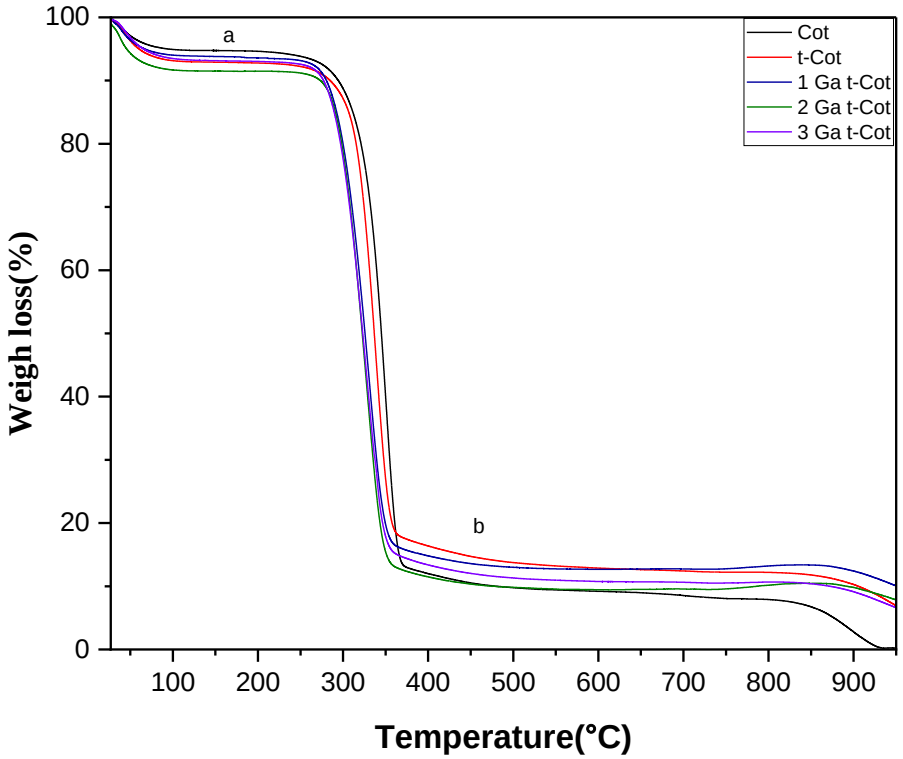

Figure 4.12. Thermograms of samples treated with $(Ga(NO_3)_3$.

4.4. ANTIBACTERIAL RESULT

The antibacterial activity of ion doped cotton groups was evaluated using the broth dilution test and sample extracts against Staphylococcus aureus. Bacterial inoculation LB Broth and LB medium were used as negative controls. Figure 4.13 shows that there was no bacterial growth in the test tubes because all ion doped groups had equal absorbance values with LB Broth. However, the pure cotton group had a higher optical density than the control LB Broth, indicating that the turbidity had increased due to the presence of developing bacteria. Inhibition of bacterial growth by ion doped groups was observed at a doping dose of 0.04 M. Lanthanum w shown to be the most effective inhibitor at increasing concentrations[169]. It has also been shown that high concentrations of $Ga(NO_3)$ have an inhibiting antibacterial effect[170]. Nanomaterials based on cobalt have the potential to not only operate as agents that directly suppress bacterial growth, but also as medication carriers for antibiotics and natural medicines [171].

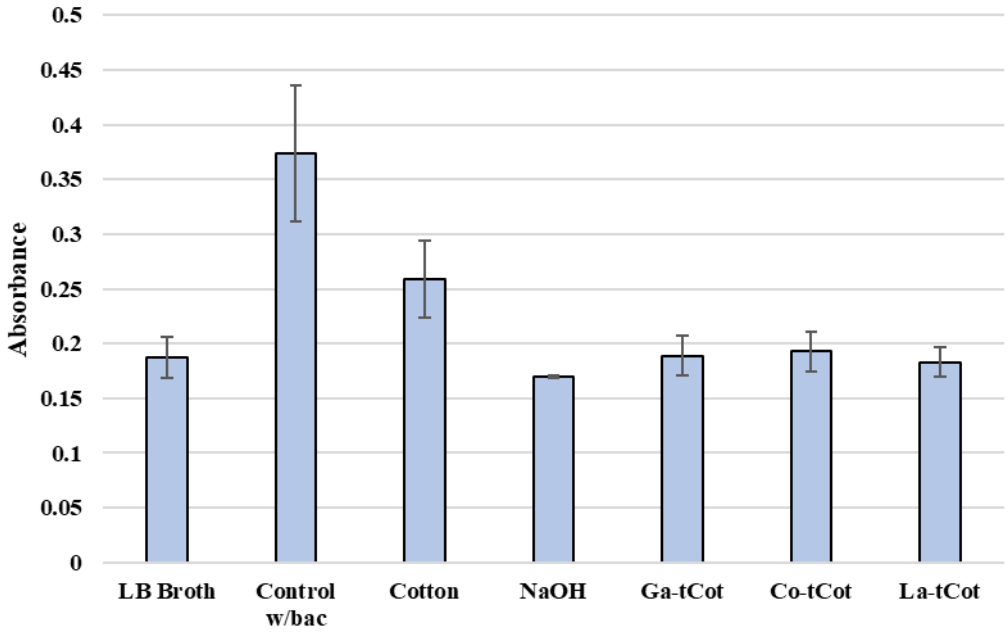

Figure 4.13. Optical densities of sample treated with Staphylococcus aureus.

A disk diffusion test called staphylococcus aureus was carried out in a further extension. The tests presented in Figure 4.14 demonstrate that none of the groups examined displayed any discernible antibacterial activity. This indicates that the ions in the cotton samples are not being leached out of the cotton effectively. Because cotton could not be properly pressed into the shape of a disk, this may be because the samples had an irregular thick three-dimensional shape with surface sections that were not in contact with the agar when only the bottom filaments of cotton were in contact with the agar, the amount of ion diffusion that occurred into the agar was inadequate to produce an inhibitory zone.

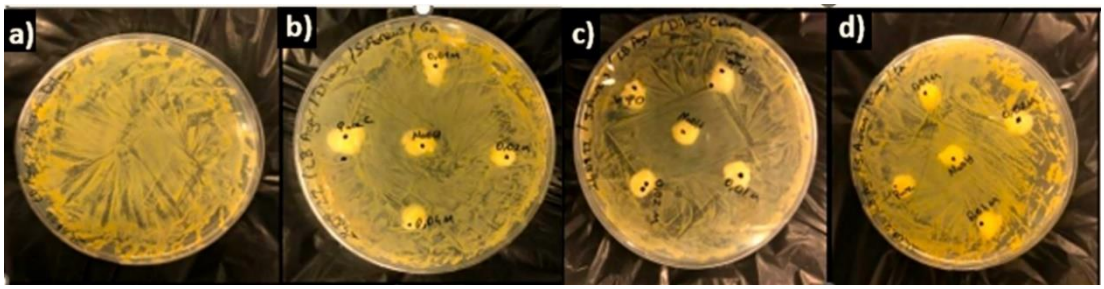

Figure 4.14. Disk diffusion test conducted with Staphylococcus aureus bacteria; a) Control Group b) 0.01, 0.02M, 0.04M Gallium c) 0.01M, 0.02M, 0.04M Cobalt d) 0.01M, 0.02M, 0.04M Lanthanum samples.

4.5. CYTOTOXICITY RESULT

Cell viability was tested after 3 and 7 days of incubation with the mouse fibroblast cell line L929. If the elements Ga, Co, and La had less than 70% cell viability, it would have indicated cytotoxicity. Figure 4.15 shows that all doped groups had higher cell viability after three days than the control group (Pure cotton). Ga $(NO_3)_3$ treatment at 1, 2, and 4 mg/mL was reported in a prior study to have maintained cell viability.[172]. However, after seven days of incubation (figure 4.16), Ga3+ ion concentrations negatively impacted cell survival, while cell viability in the Co^{3+} and La-doped groups hovered around 70% after 3 and 7 days of incubation in the total of incubations days, La^{3+} resulted in higher cell viability than the other samples.

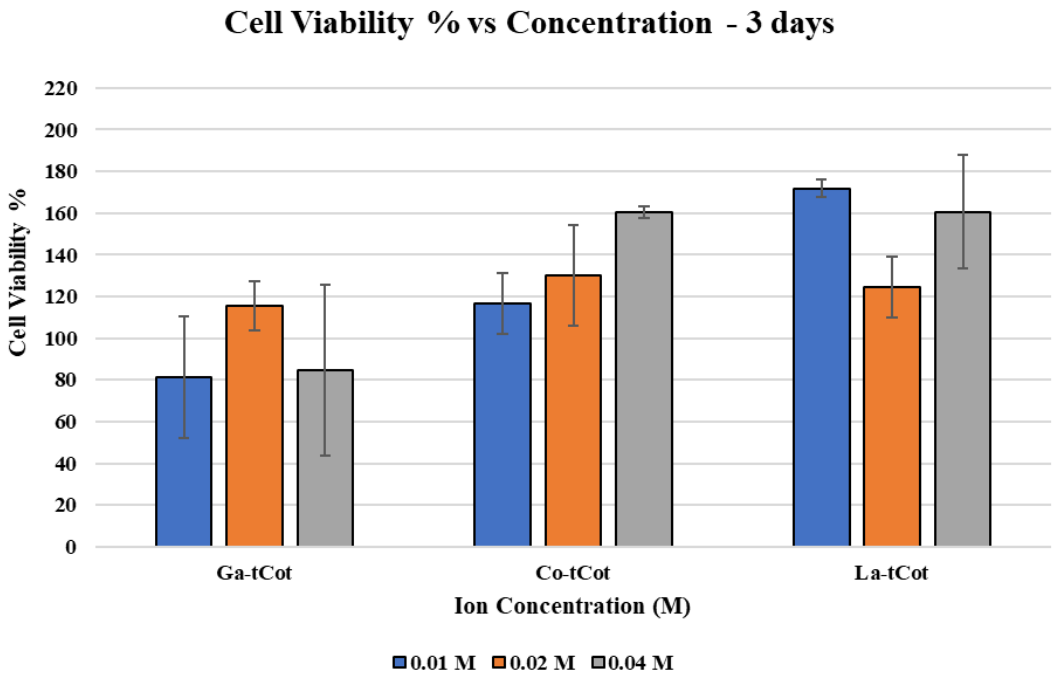

Figure 4.15. Cell viability of sample after 3 days of incubation.

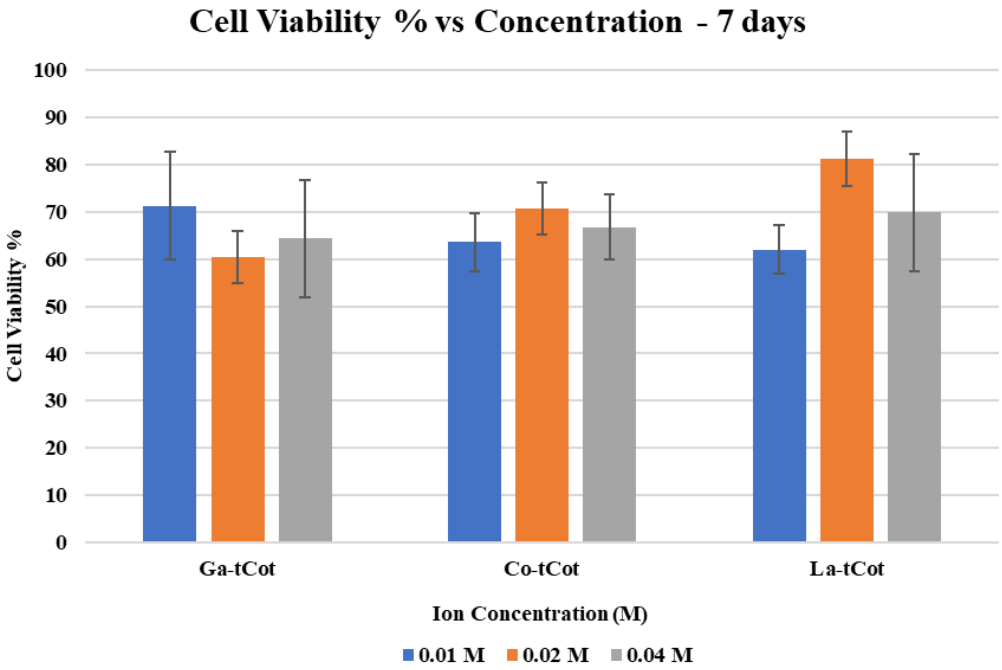

Figure 4.16. Cell viability of sample after 7 days of incubation.

CHAPTER 5

CONCLUSION AND RECOMMENDATIONS FOR FUTURE WORKS

5.1. FINDINGS OF THE THESIS

The nanoparticles-coated cotton fabric was characterized in detail by employing various techniques. The XRD pattern revealed the existence of Ga in the sample subjected to the treatment, but the distinctive reflections of La and Co metals were absent. This suggests that the peaks may have been faint and difficult to differentiate. The FTIR spectra provide some evidence that the alkali treatment of the fibres caused the conversion from cellulose I to cellulose II. In addition, the spectra provide evidence of the presence of metal oxide, so establishing the occurrence of La, Co and Ga, the activation of the cotton fibre's negative zeta potential through processing ahead of it in aqueous alkali solutions is a simple technique that facilitates cotton fabric that can be used to apply metal nanoparticles via precipitation methods. The findings of the EDX analysis demonstrated and determined that the chemical elements handled on the cotton are present in the sample. Additionally, the relative abundance of the La, Co, and Ga is proportional to the rise in the ion concentration. SEM pictures have shown that the surface of nano coated cotton contains different type of nanoparticles with the same resolution which is confirmation that the La, Co, and Ga nanoparticles were adsorbed on the cotton fabric. The TGA demonstrated nearly identical stages of combustion behaviour between the cotton covered with the ions. This thesis aimed to investigate the potential of La, Co, and Ga as novel antibacterial elements in medical cotton and textiles by coating the metal ions on cotton II. *Staphylococcus aureus* was used in the test tubes and the disc diffusion experiment to evaluate the antibacterial properties of La, Co, and Ga nanoparticles at varying concentrations. The test tube did not exhibit any turbidity for the cotton coated with ions; nonetheless, the disk diffusion assay did not demonstrate any antibacterial activity with the coated ions. It is possible that nanoparticles were likely present in the cotton. Still, insufficient nanoparticles

were present outside the cotton, resulting in an uneven distribution of nanoparticles that limited the diffusion of the ions, which could be why there is no antibacterial activity in the diffusion disk. Viable cell density profiles for the La-treated samples showed higher cell viability at the high concentration. Still, Ga also had a positive effect at low concentrations. Co had the slightly less cell viability. Still, overall, no significant drop in cell viability could be attributed to the ions maintaining metabolic activity around without substantially toxic effects on the fibroblasts.

5.2. SUGGESTED FUTURE WORK

Since cytotoxicity is a significant concern when applying nanomaterials in biomedical settings, it's encouraging to know that La, Co, and Ga nanomaterials pose no threat to healthy cells. This fabric treatment would be suitable for use in large-scale medical textile treatment facilities due to the ease with which it could be applied, the ready availability on an industrial scale, and the non-toxic nature of the components that make it up. Utilizing alternative coating techniques that use Lanthanum, Cobalt, or Gallium as the active ingredient Coating fabrics is a practical technique that may be applied to materials of any length. Its low price and simplicity make it suitable for business use.

REFERENCES

[1] A. Baroni, E. Buommino, V. De Gregorio, E. Ruocco, V. Ruocco, and R. Wolf, "Structure and function of the epidermis related to barrier properties," *Clinics in Dermatology*, vol. 30, no. 3. 2012. doi: 10.1016/j.clindermatol.2011.08.007.

[2] L. D. Renner and D. B. Weibel, "Renner, L. D.; Weibel, D. B. Physicochemical Regulation of Biofilm Formation. MRS Bull. 2011, 36, 347– 355, DOI: 10.1557/mrs.2011.65," *MRS Bulletin*, vol. 36, no. 5. 2011.

[3] I. J. Wang and J. Y. Wang, "Children with atopic dermatitis show clinical improvement after Lactobacillus exposure," *Clinical and Experimental Allergy*, vol. 45, no. 4, 2015, doi: 10.1111/cea.12489.

[4] M. Shahriari-Khalaji, A. Alassod, and Z. Nozhat, "Cotton-based health care textile: a mini review," *Polymer Bulletin*, vol. 79, no. 12. 2022. doi: 10.1007/s00289-021-04015-y.

[5] H. Hajimirzababa, R. Khajavi, M. Mirjalili, and M. KarimRahimi, "Modified cotton gauze with nano-Ag decorated alginate microcapsules and chitosan loaded with PVP-I," *Journal of the Textile Institute*, vol. 109, no. 5, 2018, doi: 10.1080/00405000.2017.1365398.

[6] D. Elieh-Ali-Komi and M. R. Hamblin, "Chitin and Chitosan: Production and Application of Versatile Biomedical Nanomaterials.," *Int J Adv Res (Indore)*, vol. 4, no. 3, 2016.

[7] S. Zivanovic, C. C. Basurto, S. Chi, P. M. Davidson, and J. Weiss, "Molecular weight of chitosan influences antimicrobial activity in oil-in-water emulsions," *J Food Prot*, vol. 67, no. 5, 2004, doi: 10.4315/0362-028X-67.5.952.

[8] K. F. El-Tahlawy, M. A. El-Bendary, A. G. Elhendawy, and S. M. Hudson, "The antimicrobial activity of cotton fabrics treated with different crosslinking agents and chitosan," *Carbohydr Polym*, vol. 60, no. 4, 2005, doi: 10.1016/j.carbpol.2005.02.019.

[9] S. Wüpper, K. Lüersen, and G. Rimbach, "Cyclodextrins, natural compounds, and plant bioactives—a nutritional perspective," *Biomolecules*, vol. 11, no. 3. 2021. doi: 10.3390/biom11030401.

[10] N. Singh and O. Sahu, "Sustainable cyclodextrin in textile applications," in *The Impact and Prospects of Green Chemistry for Textile Technology*, 2018. doi: 10.1016/B978-0-08-102491-1.00004-6.

[11] M. Orhan, “Determination and characterization of triclosan on polyethylene terephthalate fibers,” *Tekstil ve Muhendis*, vol. 19, no. 85, 2012, doi: 10.7216/130075992012198506.

[12] V. A. Dorugade and K. Bhagyashri, “Antimicrobial finishing of textiles,” *Man-Made Textiles in India*, vol. 53, no. 3. 2010.

[13] J. Davies, D. Davies, J. Davies, and D. Davies, “Origins and Evolution of Antibiotic Resistance Origins and Evolution of Antibiotic Resistance,” *Microbiology and Molecular Biology Reviews*, vol. 74, no. 3, 2010.

[14] R. G. Pearson, “Hard and Soft Acids and Bases,” *J Am Chem Soc*, vol. 85, no. 22, 1963, doi: 10.1021/ja00905a001.

[15] D. J. Burleson, M. D. Driessen, and R. L. Penn, “On the characterization of environmental nanoparticles,” *J Environ Sci Health A Tox Hazard Subst Environ Eng*, vol. 39, no. 10, 2004, doi: 10.1081/ESE-200027029.

[16] J. R. P. Jorge, V. A. Barão, J. A. Delben, L. P. Faverani, T. P. Queiroz, and W. G. Assunção, “Titanium in Dentistry: Historical development, state of the art and future perspectives,” *Journal of Indian Prosthodontist Society*, vol. 13, no. 2. 2013. doi: 10.1007/s13191-012-0190-1.

[17] M. Montazer, A. Zille, and B. Mehravani, “Synthesis and Characterization of Silver-Chitosan Nanoparticles on Textiles”, doi: 10.13140/RG.2.2.15549.79844.

[18] G. Franci *et al.*, “Silver nanoparticles as potential antibacterial agents,” *Molecules*, vol. 20, no. 5. 2015. doi: 10.3390/molecules20058856.

[19] M. R. Broadley, P. J. White, J. P. Hammond, I. Zelko, and A. Lux, “Zinc in plants: Tansley review,” *New Phytologist*, vol. 173, no. 4. 2007. doi: 10.1111/j.1469-8137.2007.01996.x.

[20] R. Jain, S. Srivastava, S. Solomon, A. K. Shrivastava, and A. Chandra, “Impact of excess zinc on growth parameters, cell division, nutrient accumulation, photosynthetic pigments and oxidative stress of sugarcane (saccharum spp.),” *Acta Physiol Plant*, vol. 32, no. 5, 2010, doi: 10.1007/s11738-010-0487-9.

[21] I. Perelshtein *et al.*, “Making the hospital a safer place by sonochemical coating of all its textiles with antibacterial nanoparticles,” *Ultrason Sonochem*, vol. 25, no. 1, 2015, doi: 10.1016/j.ultsonch.2014.12.012.

[22] A. Yadav *et al.*, “Functional finishing in cotton fabrics using zinc oxide nanoparticles,” in *Bulletin of Materials Science*, 2006. doi: 10.1007/s12034-006-0017-y.

[23] B. Balasubramaniam *et al.*, “Antibacterial and Antiviral Functional Materials: Chemistry and Biological Activity toward Tackling COVID-19-like Pandemics,” *ACS Pharmacology and Translational Science*, vol. 4, no. 1. 2021. doi: 10.1021/acsptsci.0c00174.

[24] B. Balusamy, Y. G. Kandhasamy, A. Senthamizhan, G. Chandrasekaran, M. S. Subramanian, and T. S. Kumaravel, "Characterization and bacterial toxicity of lanthanum oxide bulk and nanoparticles," *Journal of Rare Earths*, vol. 30, no. 12, 2012, doi: 10.1016/S1002-0721(12)60224-5.

[25] C. E. Arnold, A. Bordin, S. D. Lawhon, M. C. Libal, L. R. Bernstein, and N. D. Cohen, "Antimicrobial activity of gallium maltolate against Staphylococcus aureus and methicillin-resistant S. aureus and Staphylococcus pseudintermedius: An in vitro study," *Vet Microbiol*, vol. 155, no. 2–4, 2012, doi: 10.1016/j.vetmic.2011.09.009.

[26] E. L. Chang, C. Simmers, and D. A. Knight, "Cobalt complexes as antiviral and antibacterial agents," *Pharmaceuticals*, vol. 3, no. 6. 2010. doi: 10.3390/ph3061711.

[27] J. Parada, A. M. Atria, G. Wiese, E. Rivas, and G. Corsini, "Synthesis, characterization and antibacterial activity of cobalt(III) complex with phenanthroline and maltose," *Journal of the Chilean Chemical Society*, vol. 59, no. 4, 2015, doi: 10.4067/s0717-97072014000400002.

[28] B. T. Wagaye, B. F. Adamu, and A. K. Jhatial, "Recycled Cotton Fibers for Melange Yarn Manufacturing," 2020. doi: 10.1007/978-981-15-9169-3_21.

[29] D. Lebeaux, J.-M. Ghigo, and C. Beloin, "Biofilm-Related Infections: Bridging the Gap between Clinical Management and Fundamental Aspects of Recalcitrance toward Antibiotics," *Microbiology and Molecular Biology Reviews*, vol. 78, no. 3, 2014, doi: 10.1128/mmbr.00013-14.

[30] B. Gadi and G. Jeffrey, "Copper, An Ancient Remedy Returning to Fight Microbial, Fungal and Viral Infections," *Curr Chem Biol*, vol. 3, 2009.

[31] J. W. Alexander, "History of the medical use of silver," *Surgical Infections*, vol. 10, no. 3. 2009. doi: 10.1089/sur.2008.9941.

[32] C. González-Bello, "Antibiotic adjuvants – A strategy to unlock bacterial resistance to antibiotics," *Bioorg Med Chem Lett*, vol. 27, no. 18, pp. 4221–4228, Sep. 2017, doi: 10.1016/J.BMCL.2017.08.027.

[33] A. Azam, A. S. Ahmed, M. Oves, M. S. Khan, and A. Memic, "Size-dependent antimicrobial properties of CuO nanoparticles against Gram-positive and -negative bacterial strains," *Int J Nanomedicine*, vol. 7, 2012, doi: 10.2147/IJN.S29020.

[34] O. V. Zakharova, A. Y. Godymchuk, A. A. Gusev, S. I. Gulchenko, I. A. Vasyukova, and D. V. Kuznetsov, "Considerable Variation of Antibacterial Activity of Cu Nanoparticles Suspensions Depending on the Storage Time, Dispersive Medium, and Particle Sizes," *Biomed Res Int*, vol. 2015, 2015, doi: 10.1155/2015/412530.

[35] K. B. Holt and A. J. Bard, "Interaction of silver(I) ions with the respiratory chain of Escherichia coli: An electrochemical and scanning electrochemical

microscopy study of the antimicrobial mechanism of micromolar Ag," *Biochemistry*, vol. 44, no. 39, 2005, doi: 10.1021/bi0508542.

[36] K. A., P. A.K., S. S.S., S. R., and D. A., "Engineered ZnO and TiO2 nanoparticles induce oxidative stress and DNA damage leading to reduced viability of Escherichia coli," *Free Radic Biol Med*, vol. 51, no. 10, 2011.

[37] N. Esfandiari, A. Simchi, and R. Bagheri, "Size tuning of Ag-decorated TiO2 nanotube arrays for improved bactericidal capacity of orthopedic implants," *J Biomed Mater Res A*, vol. 102, no. 8, 2014, doi: 10.1002/jbm.a.34934.

[38] S. H. Cha, J. Hong, M. McGuffie, B. Yeom, J. S. Vanepps, and N. A. Kotov, "Shape-Dependent Biomimetic Inhibition of Enzyme by Nanoparticles and Their Antibacterial Activity," *ACS Nano*, vol. 9, no. 9, 2015, doi: 10.1021/acsnano.5b03247.

[39] G. R. A. A. R. S. M. K. V. G. E. G. K. C. Z. A. A. V. K. Rajukumar, "Fungus-mediated biosynthesis and characterization of TiO2 nanoparticles and their activity against pathogenic bacteria," *Spectrochimica Acta Part A:Molecular and Biomolecular Spectroscopy*, vol. 91, pp. 23–29, 2012.

[40] I. V. Sukhorukova *et al.*, "Toward bioactive yet antibacterial surfaces," *Colloids Surf B Biointerfaces*, vol. 135, 2015, doi: 10.1016/j.colsurfb.2015.06.059.

[41] L. Wang, C. Hu, and L. Shao, "The antimicrobial activity of nanoparticles: Present situation and prospects for the future," *International Journal of Nanomedicine*, vol. 12. 2017. doi: 10.2147/IJN.S121956.

[42] Y. W. Huang, C. H. Wu, and R. S. Aronstam, "Toxicity of transition metal oxide nanoparticles: Recent insights from in vitro studies," *Materials*, vol. 3, no. 10. 2010. doi: 10.3390/ma3104842.

[43] M. J. Hajipour *et al.*, "Antibacterial properties of nanoparticles," *Trends in Biotechnology*, vol. 30, no. 10. 2012. doi: 10.1016/j.tibtech.2012.06.004.

[44] T. M. Paravicini and R. M. Touyz, "NADPH oxidases, reactive oxygen species, and hypertension: clinical implications and therapeutic possibilities.," *Diabetes care*, vol. 31 Suppl 2. 2008. doi: 10.2337/dc08-s247.

[45] J. H. L. Voncken, "Physical and Chemical Properties of the Rare Earths," 2016. doi: 10.1007/978-3-319-26809-5_3.

[46] J. A. Peters, K. Djanashvili, C. F. G. C. Geraldes, and C. Platas-Iglesias, "The chemical consequences of the gradual decrease of the ionic radius along the Ln-series," *Coordination Chemistry Reviews*, vol. 406. 2020. doi: 10.1016/j.ccr.2019.213146.

[47] M. Atanassova and V. Kurteva, "Synergism as a phenomenon in solvent extraction of 4f-elements with calixarenes," *RSC Advances*, vol. 6, no. 14.

Royal Society of Chemistry, pp. 11303–11324, 2016. doi: 10.1039/c5ra22306g.

[48] L. L. Pesterfield, “Lanthanide and Actinide Chemistry (Inorganic Chemistry: A Textbook Series), 2nd Revised Edition (Cotton, Simon A.),” *J Chem Educ*, vol. 83, no. 9, 2006, doi: 10.1021/ed083p1295.

[49] J. C. G. Bünzli, “Lanthanide luminescence for biomedical analyses and imaging,” *Chem Rev*, vol. 110, no. 5, 2010, doi: 10.1021/cr900362e.

[50] S. V. Eliseeva and J. C. G. Bünzli, “Lanthanide luminescence for functional materials and bio-sciences,” *Chem Soc Rev*, vol. 39, no. 1, 2010, doi: 10.1039/b905604c.

[51] P. Prajapati, “A REVIEW: LANTHANIDE COMPLEXES AND THEIR BIOLOGICAL IMPORTANCE,” 2019, doi: 10.26479/2018.0405.56.

[52] C. X. Zhang, X. M. Qiao, H. W. Chen, and Y. Y. Zhang, “Syntheses and Biological Activities of Lanthanide Metal Complexes with Nitronly Nitroxide,” *Synthesis and Reactivity in Inorganic, Metal-Organic and Nano-Metal Chemistry*, vol. 45, no. 1, 2015, doi: 10.1080/15533174.2013.819914.

[53] Z. A. Taha, A. M. Ajlouni, and W. Al Momani, “Structural, luminescence and biological studies of trivalent lanthanide complexes with N,N′-bis(2-hydroxynaphthylmethylidene)-1,3-propanediamine Schiff base ligand,” *J Lumin*, vol. 132, no. 11, 2012, doi: 10.1016/j.jlumin.2012.05.041.

[54] Z. A. Taha, A. M. Ajlouni, W. Al Momani, and A. A. Al-Ghzawi, “Syntheses, characterization, biological activities and photophysical properties of lanthanides complexes with a tetradentate Schiff base ligand,” *Spectrochim Acta A Mol Biomol Spectrosc*, vol. 81, no. 1, 2011, doi: 10.1016/j.saa.2011.06.052.

[55] R. Gupta, N. Agrawal, and K. C. Gupta, “Synthesis, IR spectral studies and biological activities of some rare earth metal complexes with biochemically relevant ligand,” *Res J Pharm Biol Chem Sci*, vol. 3, no. 2, 2012.

[56] M. Abdus Subhan, M. Saifur Rahman, K. Alam, and M. Mahmud Hasan, “Spectroscopic analysis, DNA binding and antimicrobial activities of metal complexes with phendione and its derivative,” *Spectrochim Acta A Mol Biomol Spectrosc*, vol. 118, 2014, doi: 10.1016/j.saa.2013.09.110.

[57] K. Mohanan and S. N. Devi, “Synthesis, characterization, thermal stability, reactivity, and antimicrobial properties of some novel lanthanide(III) complexes of 2-(N-salicylideneamino)-3-carboxyethyl-4,5,6,7-tetrahydrobenzo[b]thiophene,” *Russian Journal of Coordination Chemistry/Koordinatsionnaya Khimiya*, vol. 32, no. 8, 2006, doi: 10.1134/S1070328406080124.

[58] G. Karthikeyan, K. Mohanraj, K. P. Elango, and K. Girishkumar, “Synthesis, spectroscopic characterization and antibacterial activity of lanthanide-

tetracycline complexes," *Transition Metal Chemistry*, vol. 29, no. 1, 2004, doi: 10.1023/B:TMCH.0000014490.54611.5a.

[59] S. Wang, "Cobalt - Its recovery, recycling, and application," *JOM*, vol. 58, no. 10. 2006. doi: 10.1007/s11837-006-0201-y.

[60] G. Gunn, *Critical Metals Handbook*. Wiley, 2014. doi: 10.1002/9781118755341.

[61] *The Chemistry of Iron, Cobalt and Nickel*. 1973. doi: 10.1016/c2013-0-02680-1.

[62] S. Muhammad *et al.*, "Selective extraction of heavy metals (Fe, Co, Ni) from their aqueous mixtures by Task-Specific salicylate functionalized imidazolium based ionic liquid," *J Clean Prod*, vol. 344, 2022, doi: 10.1016/j.jclepro.2022.131119.

[63] D. Osman, A. Cooke, T. R. Young, E. Deery, N. J. Robinson, and M. J. Warren, "The requirement for cobalt in vitamin B12: A paradigm for protein metalation," *Biochimica et Biophysica Acta - Molecular Cell Research*, vol. 1868, no. 1. 2021. doi: 10.1016/j.bbamcr.2020.118896.

[64] B. Uprety, R. Chandran, C. Arderne, and H. Abrahamse, "Anticancer Activity of Urease Mimetic Cobalt (III) Complexes on A549-Lung Cancer Cells: Targeting the Acidic Microenvironment," *Pharmaceutics*, vol. 14, no. 1, 2022, doi: 10.3390/pharmaceutics14010211.

[65] M. R. Karekal, V. Biradar, and M. Bennikallu Hire Mathada, "Synthesis, characterization, antimicrobial, DNA cleavage, and antioxidant studies of some metal complexes derived from Schiff base containing indole and quinoline moieties," *Bioinorg Chem Appl*, vol. 2013, 2013, doi: 10.1155/2013/315972.

[66] A. A. Abass, W. A. M. Abdulridha, W. K. Alaarage, N. H. Abdulrudha, and J. Haider, "Evaluating the antibacterial effect of cobalt nanoparticles against multi-drug resistant pathogens," *J Med Life*, vol. 14, no. 6, 2021, doi: 10.25122/jml-2021-0270.

[67] A. Bhattacharjee, A. Gupta, M. Prem Anand, P. Sengupta, A. Pandey, and T. K. Bhattacharya, "Adsorption effect of Zn+2 and Co+2 on the antibacterial properties of SiC-porcelain ceramics," *Int J Appl Ceram Technol*, vol. 17, no. 1, 2020, doi: 10.1111/ijac.13303.

[68] E. Zhang, X. Zhao, J. Hu, R. Wang, S. Fu, and G. Qin, "Antibacterial metals and alloys for potential biomedical implants," *Bioactive Materials*, vol. 6, no. 8. 2021. doi: 10.1016/j.bioactmat.2021.01.030.

[69] E. Tacconelli *et al.*, "Discovery, research, and development of new antibiotics: the WHO priority list of antibiotic-resistant bacteria and tuberculosis," *Lancet Infect Dis*, vol. 18, no. 3, 2018, doi: 10.1016/S1473-3099(17)30753-3.

[70] G. V. Vimbela, S. M. Ngo, C. Fraze, L. Yang, and D. A. Stout, "Antibacterial properties and toxicity from metallic nanomaterials," *International Journal of Nanomedicine*, vol. 12. 2017. doi: 10.2147/IJN.S134526.

[71] D. Kharade Suvarta, H. Nikam Gurunath, J. Mane Gavade Shubhangi, R. Patil Sachinkumar, and V. Gaikwad Kishor, "Biogenic synthesis of Cobalt nanopaticles using Hibiscus cannabinus leaf extract and their antibacterial activity," *Res J Chem Environ*, vol. 24, no. 5, 2020.

[72] M. Hafeez *et al.*, "Green synthesis of cobalt oxide nanoparticles for potential biological applications," *Mater Res Express*, vol. 7, no. 2, 2020, doi: 10.1088/2053-1591/ab70dd.

[73] Z. Li, J. Ma, J. Ruan, and X. Zhuang, "Using Positively Charged Magnetic Nanoparticles to Capture Bacteria at Ultralow Concentration," *Nanoscale Res Lett*, vol. 14, 2019, doi: 10.1186/s11671-019-3005-z.

[74] M. Rethinasabapathy *et al.*, "Quaternary PtRuFeCo nanoparticles supported N-doped graphene as an efficient bifunctional electrocatalyst for low-temperature fuel cells," *Journal of Industrial and Engineering Chemistry*, vol. 69, 2019, doi: 10.1016/j.jiec.2018.09.043.

[75] I. C. Kong, K. S. Ko, and D. C. Koh, "Evaluation of the effects of particle sizes of silver nanoparticles on various biological systems," *Int J Mol Sci*, vol. 21, no. 22, 2020, doi: 10.3390/ijms21228465.

[76] E. Hoseinzadeh *et al.*, "A Review on Nano-Antimicrobials: Metal Nanoparticles, Methods and Mechanisms," *Curr Drug Metab*, vol. 18, no. 2, 2016, doi: 10.2174/1389200217666161201111146.

[77] F. Tanvir, A. Yaqub, S. Tanvir, and W. A. Anderson, "Poly-l-arginine coated silver nanoprisms and their anti-bacterial properties," *Nanomaterials*, vol. 7, no. 10, 2017, doi: 10.3390/nano7100296.

[78] R. R. Moskalyk, "Gallium: The backbone of the electronics industry," *Miner Eng*, vol. 16, no. 10, 2003, doi: 10.1016/j.mineng.2003.08.003.

[79] S. Kumar, C. Tessarek, S. Christiansen, and R. Singh, "A comparative study of Ga2O3 nanowires grown on different substrates using CVD technique," *J Alloys Compd*, vol. 587, 2014, doi: 10.1016/j.jallcom.2013.10.165.

[80] A. Usseinov *et al.*, "Ab-Initio Calculations of Oxygen Vacancy in Ga2O3Crystals," *Latvian Journal of Physics and Technical Sciences*, vol. 58, no. 2, pp. 3–10, Apr. 2021, doi: 10.2478/lpts-2021-0007.

[81] P. Melnikov, A. Malzac, and M. D. B. Coelho, "Gallium and bone pathology," *Acta Ortopedica Brasileira*, vol. 16, no. 1. 2008. doi: 10.1590/S1413-78522008000100011.

[82] K. DeLeon *et al.*, “Gallium maltolate treatment eradicates pseudomonas aeruginosa infection in thermally injured mice,” *Antimicrob Agents Chemother*, vol. 53, no. 4, 2009, doi: 10.1128/AAC.01330-08.

[83] L. R. Bernstein, “Mechanisms of therapeutic activity for gallium,” *Pharmacological Reviews*, vol. 50, no. 4. 1998.

[84] S. P. Valappil *et al.*, “Controlled delivery of antimicrobial gallium ions from phosphate-based glasses,” *Acta Biomater*, vol. 5, no. 4, 2009, doi: 10.1016/j.actbio.2008.09.019.

[85] C. Mellier *et al.*, “Characterization and properties of novel gallium-doped calcium phosphate ceramics,” *Inorg Chem*, vol. 50, no. 17, 2011, doi: 10.1021/ic2007777.

[86] G. Grass, C. Rensing, and M. Solioz, “Metallic copper as an antimicrobial surface,” *Applied and Environmental Microbiology*, vol. 77, no. 5. 2011. doi: 10.1128/AEM.02766-10.

[87] J. A. Lemire, J. J. Harrison, and R. J. Turner, “Antimicrobial activity of metals: Mechanisms, molecular targets and applications,” *Nature Reviews Microbiology*, vol. 11, no. 6. 2013. doi: 10.1038/nrmicro3028.

[88] S. Prabhu and E. K. Poulose, “Silver nanoparticles: mechanism of antimicrobial action, synthesis, medical applications, and toxicity effects,” *Int Nano Lett*, vol. 2, no. 1, 2012, doi: 10.1186/2228-5326-2-32.

[89] S. Shleev *et al.*, “Direct electron transfer between copper-containing proteins and electrodes,” *Biosensors and Bioelectronics*, vol. 20, no. 12. 2005. doi: 10.1016/j.bios.2004.10.003.

[90] L. Sintubin *et al.*, “Lactic acid bacteria as reducing and capping agent for the fast and efficient production of silver nanoparticles,” *Appl Microbiol Biotechnol*, vol. 84, no. 4, 2009, doi: 10.1007/s00253-009-2032-6.

[91] M. Nita and A. Grzybowski, “The Role of the Reactive Oxygen Species and Oxidative Stress in the Pathomechanism of the Age-Related Ocular Diseases and Other Pathologies of the Anterior and Posterior Eye Segments in Adults,” *Oxidative Medicine and Cellular Longevity*, vol. 2016. 2016. doi: 10.1155/2016/3164734.

[92] Y. Qing *et al.*, “Potential antibacterial mechanism of silver nanoparticles and the optimization of orthopedic implants by advanced modification technologies,” *International Journal of Nanomedicine*, vol. 13. 2018. doi: 10.2147/IJN.S165125.

[93] Y. Kaneko, M. Thoendel, O. Olakanmi, B. E. Britigan, and P. K. Singh, “The transition metal gallium disrupts Pseudomonas aeruginosa iron metabolism and has antimicrobial and antibiofilm activity,” *Journal of Clinical Investigation*, vol. 117, no. 4, 2007, doi: 10.1172/JCI30783.

[94] O. Olakanmi, B. E. Britigan, and L. S. Schlesinger, “Gallium disrupts iron metabolism of mycobacteria residing within human macrophages,” *Infect Immun*, vol. 68, no. 10, 2000, doi: 10.1128/IAI.68.10.5619-5627.2000.

[95] C. R. Chitambar and J. Narasimhan, “Targeting iron-dependent DNA synthesis with gallium and transferrin-gallium,” *Pathobiology*, vol. 59, no. 1, 1991, doi: 10.1159/000163609.

[96] J. R. Harrington, R. J. Martens, N. D. Cohen, and L. R. Bernstein, “Antimicrobial activity of gallium against virulent Rhodococcus equiin vitro and in vivo,” *J Vet Pharmacol Ther*, vol. 29, no. 2, 2006, doi: 10.1111/j.1365-2885.2006.00723.x.

[97] G. Eby, “Elimination of arthritis pain and inflammation for over 2 years with a single 90 min, topical 14% gallium nitrate treatment: Case reports and review of actions of gallium III,” *Med Hypotheses*, vol. 65, no. 6, 2005, doi: 10.1016/j.mehy.2005.06.021.

[98] C. H. Goss *et al.*, “Gallium disrupts bacterial iron metabolism and has therapeutic effects in mice and humans with lung infections,” *Sci Transl Med*, vol. 10, no. 460, 2018, doi: 10.1126/scitranslmed.aat7520.

[99] P. Melnikov, A. Malzac, and M. D. B. Coelho, “Gallium and bone pathology,” *Acta Ortop Bras*, vol. 16, no. 1, pp. 54–57, 2008, doi: 10.1590/S1413-78522008000100011.

[100] T. D. Coates, “Physiology and pathophysiology of iron in hemoglobin-associated diseases,” *Free Radical Biology and Medicine*, vol. 72. 2014. doi: 10.1016/j.freeradbiomed.2014.03.039.

[101] C. R. Chitambar, “The therapeutic potential of iron-targeting gallium compounds in human disease: From basic research to clinical application,” *Pharmacological Research*, vol. 115. 2017. doi: 10.1016/j.phrs.2016.11.009.

[102] O. Rzhepishevska *et al.*, “The antibacterial activity of Ga3+ is influenced by ligand complexation as well as the bacterial carbon source,” *Antimicrob Agents Chemother*, vol. 55, no. 12, 2011, doi: 10.1128/AAC.00386-11.

[103] M. Kurtjak, M. Vukomanović, L. Kramer, and D. Suvorov, “Biocompatible nano-gallium/hydroxyapatite nanocomposite with antimicrobial activity,” *J Mater Sci Mater Med*, vol. 27, no. 11, 2016, doi: 10.1007/s10856-016-5777-3.

[104] P. Wang, L. Zhao, J. Liu, M. D. Weir, X. Zhou, and H. H. K. Xu, “Bone tissue engineering via nanostructured calcium phosphate biomaterials and stem cells,” *Bone Research*, vol. 2. 2015. doi: 10.1038/boneres.2014.17.

[105] I. M. El Nahhal, A. A. Elmanama, and N. M. Amara, “Synthesis of Nanometal Oxide–Coated Cotton Composites,” in *Cotton Research*, 2016. doi: 10.5772/63505.

[106] A. P. Periyasamy, M. Venkataraman, D. Kremenakova, J. Militky, and Y. Zhou, “Progress in sol-gel technology for the coatings of fabrics,” *Materials*, vol. 13, no. 8, 2020, doi: 10.3390/MA13081838.

[107] S. Esposito, “‘Traditional’ sol-gel chemistry as a powerful tool for the preparation of supported metal and metal oxide catalysts,” *Materials*, vol. 12, no. 4. 2019. doi: 10.3390/ma12040668.

[108] F. A. Shalahuddin, S. S. Almekahdinah, and A. B. D. Nandiyanto, “Preliminary Economic Study on the Production of ZnO Nanoparticles Using a Sol-Gel Synthesis Method,” *Jurnal Kimia Terapan Indonesia*, vol. 21, no. 1, 2019, doi: 10.14203/jkti.v21i1.407.

[109] A. E. Danks, S. R. Hall, and Z. Schnepp, “The evolution of ‘sol-gel’ chemistry as a technique for materials synthesis,” *Mater Horiz*, vol. 3, no. 2, 2016, doi: 10.1039/c5mh00260e.

[110] D. Bokov *et al.*, “Nanomaterial by Sol-Gel Method: Synthesis and Application,” *Advances in Materials Science and Engineering*, vol. 2021. 2021. doi: 10.1155/2021/5102014.

[111] O. Carp, C. L. Huisman, and A. Reller, “Photoinduced reactivity of titanium dioxide,” *Progress in Solid State Chemistry*, vol. 32, no. 1–2. Elsevier Ltd, pp. 33–177, 2004. doi: 10.1016/j.progsolidstchem.2004.08.001.

[112] A. Gedanken, “Doping nanoparticles into polymers and ceramics using ultrasound radiation,” *Ultrason Sonochem*, vol. 14, no. 4, 2007, doi: 10.1016/j.ultsonch.2006.08.005.

[113] “Dekker encyclopedia of nanoscience and nanotechnology,” *Choice Reviews Online*, vol. 42, no. 05, 2005, doi: 10.5860/choice.42-2552.

[114] P. R. Chang, R. Jian, P. Zheng, J. Yu, and X. Ma, “Preparation and properties of glycerol plasticized-starch (GPS)/cellulose nanoparticle (CN) composites,” *Carbohydr Polym*, vol. 79, no. 2, 2010, doi: 10.1016/j.carbpol.2009.08.007.

[115] P. R. Chang, R. Jian, J. Yu, and X. Ma, “Starch-based composites reinforced with novel chitin nanoparticles,” *Carbohydr Polym*, vol. 80, no. 2, 2010, doi: 10.1016/j.carbpol.2009.11.041.

[116] J. Gong, J. Li, J. Xu, Z. Xiang, and L. Mo, “Research on cellulose nanocrystals produced from cellulose sources with various polymorphs,” *RSC Adv*, vol. 7, no. 53, 2017, doi: 10.1039/c7ra06222b.

[117] M. Wada, H. Chanzy, Y. Nishiyama, and P. Langan, “Cellulose III I crystal structure and hydrogen bonding by synchrotron X-ray and neutron fiber diffraction,” *Macromolecules*, vol. 37, no. 23, pp. 8548–8555, Nov. 2004, doi: 10.1021/ma0485585.

[118] P. Mansikkamäki, M. Lahtinen, and K. Rissanen, “The conversion from cellulose I to cellulose II in NaOH mercerization performed in alcohol-water

systems: An X-ray powder diffraction study," *Carbohydr Polym*, vol. 68, no. 1, 2007, doi: 10.1016/j.carbpol.2006.07.010.

[119] P. E. S. Silva, R. Chagas, S. N. Fernandes, P. Pieranski, R. L. B. Selinger, and M. H. Godinho, "Travelling colourful patterns in self-organized cellulose-based liquid crystalline structures," *Commun Mater*, vol. 2, no. 1, 2021, doi: 10.1038/s43246-021-00182-7.

[120] F. G. Pearson, R. H. Marchessault, and C. Y. Liang, "Infrared spectra of crystalline polysaccharides. V. Chitin," *Journal of Polymer Science*, vol. 43, no. 141, 1960, doi: 10.1002/pol.1960.1204314109.

[121] U. J. Kim, Y. R. Lee, T. H. Kang, J. W. Choi, S. Kimura, and M. Wada, "Protein adsorption of dialdehyde cellulose-crosslinked chitosan with high amino group contents," *Carbohydr Polym*, vol. 163, 2017, doi: 10.1016/j.carbpol.2017.01.052.

[122] P. Garside and P. Wyeth, "Maney Publishing International Institute for Conservation of Historic and Artistic Works Identification of Cellulosic Fibres by FTIR Spectroscopy: Thread and Single Fibre Analysis by Attenuated Total Reflectance," 2003. [Online]. Available: http://www.jstor.orgURL:http://www.jstor.org/stable/1506916

[123] S. R. Ankireddy and J. Kim, "Selective detection of dopamine in the presence of ascorbic acid via fluorescence quenching of inp/zns quantum dots," *Int J Nanomedicine*, vol. 10, 2015, doi: 10.2147/IJN.S88388.

[124] W. A. Dick, D. Kost, and L. Chen, "Availability of sulfur to crops from soil and other sources," in *Sulfur: A Missing Link between Soils, Crops, and Nutrition*, 2015. doi: 10.2134/agronmonogr50.c5.

[125] S. M. L. Silva, C. R. C. Braga, M. V. L. Fook, C. M. O. Raposo, L. H. Carvalho, and E. L. Canedo, "Application of Infrared Spectroscopy to Analysis of Chitosan/Clay Nanocomposites," in *Infrared Spectroscopy - Materials Science, Engineering and Technology*, 2012. doi: 10.5772/35522.

[126] J. Li *et al.*, "Microwave-assisted solvent-free acetylation of cellulose with acetic anhydride in the presence of iodine as a catalyst," *Molecules*, vol. 14, no. 9, 2009, doi: 10.3390/molecules14093551.

[127] Y. Hishikawa, E. Togawa, and T. Kondo, "Characterization of Individual Hydrogen Bonds in Crystalline Regenerated Cellulose Using Resolved Polarized FTIR Spectra," *ACS Omega*, vol. 2, no. 4, 2017, doi: 10.1021/acsomega.6b00364.

[128] A. S. Abu-Khadra, R. S. Farag, and A. E.-D. M. Abdel-Hady, "Synthesis, Characterization and Antimicrobial Activity of Schiff Base (<i>E</i>)-<i>N</i>-(4-(2-Hydroxybenzylideneamino) Phenylsulfonyl) Acetamide Metal Complexes," *Am J Analyt Chem*, vol. 07, no. 03, 2016, doi: 10.4236/ajac.2016.73020.

[129] V. Shahedifar and A. M. Rezadoust, “Thermal and mechanical behavior of cotton/vinyl ester composites: Effects of some flame retardants and fiber treatment,” *Journal of Reinforced Plastics and Composites*, vol. 32, no. 10, 2013, doi: 10.1177/0731684413475911.

[130] B. Nabil, E. A. Ahmida, C. Christine, V. Julien, and A. Abdelkrim, “Polyfunctional cotton fabrics with catalytic activity and antibacterial capacity,” *Chemical Engineering Journal*, vol. 351, 2018, doi: 10.1016/j.cej.2018.06.050.

[131] A. D. French, “Idealized powder diffraction patterns for cellulose polymorphs,” *Cellulose*, vol. 21, no. 2, 2014, doi: 10.1007/s10570-013-0030-4.

[132] X. Zhang, X. Wang, and Z. Chen, “Radioactive cobalt(II) removal from aqueous solutions using a reusable nanocomposite: Kinetic, isotherms, and mechanistic study,” *Int J Environ Res Public Health*, vol. 14, no. 12, Dec. 2017, doi: 10.3390/ijerph14121453.

[133] A. B. D. Nandiyanto, R. Oktiani, and R. Ragadhita, “How to read and interpret ftir spectroscope of organic material,” *Indonesian Journal of Science and Technology*, vol. 4, no. 1, 2019, doi: 10.17509/ijost.v4i1.15806.

[134] Z. YILDIZ, “Investigation of Polypyrrole Coated Cotton Fabrics as Electromagnetic Shielding Material,” *MARMARA UNIVERSITY JOURNAL OF SCIENCE*, vol. 27, no. 3, 2015, doi: 10.7240/mufbed.46082.

[135] G. Pezzotti *et al.*, “Raman Spectroscopy of Oral Candida Species: Molecular-Scale Analyses, Chemometrics, and Barcode Identification,” *Int J Mol Sci*, vol. 23, no. 10, May 2022, doi: 10.3390/ijms23105359.

[136] P. Sundaramoorthi and S. Kalainathan, “Crystal growth and characterization studies of SMHP single crystal in silica gel medium and laser induced nucleation reduction process,” *Biochem Eng J*, vol. 35, no. 2, 2007, doi: 10.1016/j.bej.2006.12.027.

[137] L. Sun, L. Li, X. An, and X. Qian, “Mechanically strong, liquid-resistant photothermal bioplastic constructed from cellulose and metal-organic framework for light-driven mechanical motion,” *Molecules*, vol. 26, no. 15, 2021, doi: 10.3390/molecules26154449.

[138] T. Goto, S. Zaccaron, M. Bacher, H. Hettegger, A. Potthast, and T. Rosenau, “On nitrogen fixation and ‘residual nitrogen content’ in cellulosic pulps,” *Carbohydr Polym*, vol. 253, 2021, doi: 10.1016/j.carbpol.2020.117235.

[139] C. M. Popescu, C. Vasile, M. C. Popescu, G. Singurel, V. I. Popa, and B. S. Munteanu, “Analytical methods for lignin characterization. II. Spectroscopic studies,” *Cellulose Chemistry and Technology*, vol. 40, no. 8, 2006.

[140] J. G. Gwon, S. Y. Lee, G. H. Doh, and J. H. Kim, "Characterization of chemically modified wood fibers using FTIR spectroscopy for biocomposites," *J Appl Polym Sci*, vol. 116, no. 6, 2010, doi: 10.1002/app.31746.

[141] W. Lyu, Y. Shi, Y. Zheng, and X. Liu, "XPS and FTIR studies of fungus-stained Daemonorops margaritae," *J For Res (Harbin)*, vol. 30, no. 2, 2019, doi: 10.1007/s11676-018-0598-5.

[142] A. SAĞLAM, "Experimental and Theoretical Investigation of Molecular Structure and Vibrational Frequencies of 3-Cyano-7-hydroxycoumarin by Density Functional Theory," *Süleyman Demirel Üniversitesi Fen Bilimleri Enstitüsü Dergisi*, vol. 21, no. 3, 2017, doi: 10.19113/sdufbed.09372.

[143] A. G. Barua, S. Hazarika, M. Hussain, and A. K. Misra, "Spectroscopic Investigation of the Cashew Nut Kernel (Anacardium occidentale)," *The Open Food Science Journal*, vol. 2, no. 1, 2008, doi: 10.2174/1874256400802010085.

[144] B. Gurukarthik Babu, D. Prince Winston, P. SenthamaraiKannan, S. S. Saravanakumar, and M. R. Sanjay, "Study on characterization and physicochemical properties of new natural fiber from Phaseolus vulgaris," *Journal of Natural Fibers*, vol. 16, no. 7, 2019, doi: 10.1080/15440478.2018.1448318.

[145] M. S. R. Seetharaman and P. Sivagurunathan, "Study Of the Structural, Morphological and Magnetic Properties of Cofe2o4 Nanoparticles Prepared by Co-Precipitation Method," vol. 20, pp. 7076–7085, doi: 10.14704/nq.2022.20.6.NQ22711.

[146] W. Xing *et al.*, "Flame retardancy and thermal degradation of cotton textiles based on UV-curable flame retardant coatings," *Thermochim Acta*, vol. 513, no. 1–2, 2011, doi: 10.1016/j.tca.2010.11.014.

[147] N. Montoya-Escobar *et al.*, "Use of Fourier Series in X-ray Diffraction (XRD) Analysis and Fourier-Transform Infrared Spectroscopy (FTIR) for Estimation of Crystallinity in Cellulose from Different Sources," *Polymers (Basel)*, vol. 14, no. 23, Dec. 2022, doi: 10.3390/polym14235199.

[148] C. Trilokesh and K. B. Uppuluri, "Isolation and characterization of cellulose nanocrystals from jackfruit peel," *Sci Rep*, vol. 9, no. 1, 2019, doi: 10.1038/s41598-019-53412-x.

[149] S. Borysiak and B. Doczekalska, "X-ray Diffraction Study of Pine Wood Treated with NaOH."

[150] M. I. Chen, A. K. Singh, J. L. Chiang, R. H. Horng, and D. S. Wuu, "Zinc gallium oxide—a review from synthesis to applications," *Nanomaterials*, vol. 10, no. 11. 2020. doi: 10.3390/nano10112208.

[151] E. Gebauer-Henke, J. Farbotko, R. Touroude, and J. Rynkowski, "A comparative study of Ir/Ga2O3, Pt/Ga 2O3, and Ru/Ga2O3 catalysts in

selective hydrogenation of crotonaldehyde," in *Kinetics and Catalysis*, 2008. doi: 10.1134/S0023158408040186.

[152] I. Niskanen *et al.*, "Optical Properties of Cellulose Nanofibre Films at High Temperatures," *Journal of Polymer Research*, vol. 29, no. 5, 2022, doi: 10.1007/s10965-022-03019-0.

[153] R. O. Asriza, Ropalia, D. Humaira, G. O. Ryaldi, and Zomi, "Characterization of cellulose acetate functional groups synthesized from corn husk (Zea mays)," in *IOP Conference Series: Earth and Environmental Science*, 2021. doi: 10.1088/1755-1315/926/1/012060.

[154] D. Kocaefe, S. Poncsak, and Y. Boluk, "Effect of thermal treatment on the chemical composition and mechanical properties of birch and aspen," *BioResources*, vol. 3, no. 2. 2008.

[155] B. D. Mattos, T. V. Lourençon, L. Serrano, J. Labidi, and D. A. Gatto, "Chemical modification of fast-growing eucalyptus wood," *Wood Sci Technol*, vol. 49, no. 2, 2015, doi: 10.1007/s00226-014-0690-8.

[156] M. Schwanninger, J. C. Rodrigues, H. Pereira, and B. Hinterstoisser, "Effects of short-time vibratory ball milling on the shape of FT-IR spectra of wood and cellulose," *Vib Spectrosc*, vol. 36, no. 1, 2004, doi: 10.1016/j.vibspec.2004.02.003.

[157] T. Koyama, S. Kino, and Y. Matsuura, "Accuracy Improvement of Blood Glucose Measurement System Using Quantum Cascade Lasers," *Optics and Photonics Journal*, vol. 09, no. 10, 2019, doi: 10.4236/opj.2019.910014.

[158] M. G. Raucci *et al.*, "Effect of citric acid crosslinking cellulose-based hydrogels on osteogenic differentiation," *J Biomed Mater Res A*, vol. 103, no. 6, 2015, doi: 10.1002/jbm.a.35343.

[159] R. O. Asriza, Ropalia, D. Humaira, G. O. Ryaldi, and Zomi, "Characterization of cellulose acetate functional groups synthesized from corn husk (Zea mays)," in *IOP Conference Series: Earth and Environmental Science*, 2021. doi: 10.1088/1755-1315/926/1/012060.

[160] J. Jing Ang, T. Whye Wong, and Z. Abdul Karim, "Synthesis and characterization of two-stage curing reactive bio-based polymers," 2018.

[161] Y. Liu and H. J. Kim, "Fourier transform infrared spectroscopy (FT-IR) and simple algorithm analysis for rapid and non-destructive assessment of developmental cotton fibers," *Sensors (Switzerland)*, vol. 17, no. 7, 2017, doi: 10.3390/s17071469.

[162] C. Marutoiu, I. Bratu, A. M. Budu, G. Santa, and O. F. Marutoiu, "Evaluation of Conservation State by Analysis of Imperial Gates' Constituent Materials Belonging to A^{o}chileu Mic Wooden Church, Cluj County CALIN NEAMTU 4 , CLAUDIU TANASELIA 5 , IRINA KACSO 2 , IRINA CRINA ANCA SANDU," 2015. [Online]. Available: http://www.revistadechimie.ro

[163] M. I. Makhdum, M. Nawaz, A. Malik, I. Chaudhry, and A. Shabab-Ud-Din, “Effects of Gypsum as a Sulphur Fertilizer in Cotton (Gossypium hirsutum L.) Production.” [Online]. Available: http://www.ijab.org

[164] W. Y. Tew *et al.*, “Application of FT-IR spectroscopy and chemometric technique for the identification of three different parts of Camellia nitidissima and discrimination of its authenticated product,” *Front Pharmacol*, vol. 13, Sep. 2022, doi: 10.3389/fphar.2022.931203.

[165] G. Korotcenkov, S. Do Han, B. Cho, and V. Tolstoy, “Structural characterization and phase transformations in metal oxide fi lms synthesized by Successive Ionic Layer Deposition (SILD) method,” 2009.

[166] G. C. E, A. E. B, and N. G. I, “Thermo-gravimetry (TGA) and DSC of thermal analysis techniques in production of active carbon from lignocellulosic materials,” *Pelagia Research Library Advances in Applied Science Research*, vol. 7, no. 2, 2016.

[167] S. Ma, S. J. Yu, Z. H. Wang, and X. L. Zheng, “Ultrasound-assisted modification of beet pulp cellulose with phthalic anhydride in ionic liquid,” *Cellulose Chemistry and Technology*, vol. 47, no. 7–8, 2013.

[168] Y. Li, H. Xiao, M. Chen, Z. Song, and Y. Zhao, “Absorbents based on maleic anhydride-modified cellulose fibers/diatomite for dye removal,” in *Journal of Materials Science*, 2014. doi: 10.1007/s10853-014-8270-8.

[169] S. Guo, L. Wang, A. Lu, T. Lu, X. Ding, and X. Huang, “Inhibition mechanism of lanthanum ion on the activity of horseradish peroxidase in vitro,” *Spectrochim Acta A Mol Biomol Spectrosc*, vol. 75, no. 2, 2010, doi: 10.1016/j.saa.2009.11.033.

[170] E. Banin *et al.*, “The potential of desferrioxamine-gallium as an anti-Pseudomonas therapeutic agent,” *Proc Natl Acad Sci U S A*, vol. 105, no. 43, 2008, doi: 10.1073/pnas.0808608105.

[171] A. Bhattacharjee *et al.*, “Effect of Zn and Co doping on antibacterial efficacy and cytocompatibility of spark plasma sintered hydroxyapatite,” *Journal of the American Ceramic Society*, vol. 103, no. 8, 2020, doi: 10.1111/jace.17077.

[172] M. Mosina *et al.*, “Gallium-Doped Hydroxyapatite Shows Antibacterial Activity against Pseudomonas aeruginosa without Affecting Cell Metabolic Activity,” *J Funct Biomater*, vol. 14, no. 2, 2023, doi: 10.3390/jfb14020051.

RESUME

Ladan ABDI ATTEYE graduated from the University of Djibouti at the Department of Biology/Biochemistry in 2018. She completed her master's degree in Karabuk University Graduate Education Institute in Department of Biomedical Engineering in 2023.